

**Determination of Naturally Occurring Radioactive Elements and  
Radiation Exposure Levels in the Soapstone Quarries of Tabaka  
Region of Kisii District, Kenya**

**Vincent Otworri Atambo**

**A thesis submitted in partial fulfillment for the Degree of Master of  
Science in Physics in the Jomo Kenyatta University of Agriculture and  
Technology**

**2011**

**DECLARATION**

This thesis is my original work and has not been presented for a degree in any other university.

Signature: .....

Date: .....

**Vincent Otworì Atambo**

This thesis has been submitted for examination with our approval as University supervisors.

Signature: .....

Date: .....

**Dr. Robert Kinyua**

**JKUAT, Kenya**

Signature.....

Date:.....

**Dr. Richard M Ongerì**

**JKUAT, Kenya**

## **DEDICATION**

I dedicate this work to my dear wife Lillian, my daughters Angela and Michelle, my son Victor, my dear parents, brothers and sisters for their support, encouragement and patience during the study period.

## **ACKNOWLEDGEMENT**

I sincerely thank my supervisors, Dr. Robert Kinyua and Dr. Richard Ongeru for the great effort they put in guiding me throughout my work. My thanks also go to the Teachers Service Commission (TSC) for granting me a study leave with pay that facilitated my upkeep throughout the study period.

I greatly thank Dr. Githiri, Dr. Ngaruiya (Chairman Physics Department), Dr. Kihara and all members of the Physics Department of JKUAT for their moral support and encouragement. I also thank the staff of the Civil Engineering Department of JKUAT for allowing me to use their equipment during sample preparation.

I am also much indebted to the Chief Radiation Protection Officer, Mr Joel Kamande, radiophysicist Alice Karigi and the technical staff of National Radiation Protection Board where all the laboratory experiments were conducted, for their support and positive criticism during my study period.

Above all, my sincere thanks go to the Almighty God without whom I would not have had the strength to carry out and complete my studies.

## TABLE OF CONTENTS

<b>DECLARATION</b> .....	i
<b>DEDICATION</b> .....	ii
<b>ACKNOWLEDGEMENT</b> .....	iii
<b>TABLE OF CONTENTS</b> .....	iv
<b>LIST OF TABLES</b> .....	viii
<b>LIST OF FIGURES</b> .....	x
<b>LIST OF PLATES</b> .....	xii
<b>LIST OF APPENDICES</b> .....	xiii
<b>LIST OF ABBREVIATIONS AND ACRONYMS</b> .....	xiv
<b>LIST OF SYMBOLS</b> .....	xvii
<b>ABSTRACT</b> .....	xviii
<b>CHAPTER ONE</b> .....	1
1.0 INTRODUCTION AND LITERATURE REVIEW.....	1
1.1 INTRODUCTION .....	1
1.2 LITERATURE REVIEW.....	3
1.2.1 Earlier Studies on Terrestrial Radionuclides.....	3
1.2.2 Soapstone.....	15
1.3 GEOLOGY OF TABAKA REGION.....	16
1.4 PROBLEM STATEMENT.....	17
1.5 OBJECTIVES.....	17
1.5.1 Main Objective.....	17
1.5.2 Specific Objectives.....	18

1.6 JUSTIFICATION.....	18
<b>CHAPTER TWO</b> .....	19
<b>1.0 NATURAL RADIOACTIVITY</b> .....	19
2.1 THEORY OF NATURAL RADIOACTIVITY.....	19
2.2 RADIOACTIVE EMISSIONS .....	22
2.2.1 Gamma Ray Production.....	25
2.2.2 Units of Measurement and Exposure.....	26
2.2.3 Interaction of Gamma Rays with Matter.....	26
2.2.3.1 Photoelectric Absorption.....	28
2.2.3.2 Compton Scattering.....	30
2.2.3.3 Pair Production.....	32
2.3 EFFECTS OF IONIZING RADIATION ON CELLS .....	33
2.3.1 Health Effects of Gamma Rays.....	37
2.4 GAMMA RAY DETECTORS.....	39
2.4.1 Energy Resolution.....	43
2.4.2 Detector Efficiency .....	44
<b>CHAPTER THREE</b> .....	46
<b>2.0 MATERIALS AND METHODS</b> .....	46
3.1 SAMPLE COLLECTION.....	46
3.2 SAMPLE PREPARATION.....	49
3.3 ACTIVITY CONCENTRATION MEASUREMENTS.....	51

3.4 RADIONUCLIDE IDENTIFICATION REPORTS.....	53
3.5 ABSORBED DOSE.....	54
3.5.1 Measurement of Absorbed Dose Rates In Air.....	54
3.5.2 Calculation of Absorbed Dose Rates.....	55
3.5.3 Calculation of Annual Effective Dose.....	55
3.5.4 External Hazard Index.....	56
3.5.5 Internal Hazard Index.....	57
<b>CHAPTER FOUR.....</b>	<b>58</b>
<b>4.0 RESULTS AND DISCUSSION.....</b>	<b>58</b>
4.1 SPECTRA FOR VARIOUS SAMPLES.....	58
4.2 ACTIVITY CONCENTRATIONS OF RADIONUCLIDES IN THE SAMPLES...59	
4.3 ABSORBED DOSE RATES.....	62
4.3.1 Measured Absorbed Dose Rates.....	62
4.3.2 Calculated Absorbed Dose Rates.....	62
4.4 EXTERNAL HAZARD INDEX AND INTERNAL HAZARD INDEX.....	67
4.5 ANNUAL EFFECTIVE DOSE RATE.....	69
<b>CHAPTER FIVE.....</b>	<b>71</b>
<b>5.0 CONCLUSIONS AND RECOMMENDATIONS.....</b>	<b>71</b>
5.1 CONCLUSION.....	71
5.2 RECOMMENDATIONS.....	72

**REFERENCES**.....74

**APPENDICES**.....84

## LIST OF TABLES

<b>Table 3.1:</b> Quarry identity and sample type collected.....	46
<b>Table 3.2:</b> Identified radionuclides for IAEA – 365 soil sample.....	53
<b>Table 3.3:</b> Spectroscopic parameters employed for quantification of activity levels.....	54
<b>Table 4.1:</b> Activity of radionuclides $^{232}\text{Th}$ , $^{226}\text{Ra}$ and $^{40}\text{K}$ in the measured rock/soil samples from Tabaka soapstone quarries in Kenya.....	59
<b>Table 4.2:</b> Comparison between average activities of radionuclides in each quarry and the world average activities of the radionuclides.....	61
<b>Table 4.3:</b> Absorbed dose rates measured 1 m above the surface at each quarry.....	62
<b>Table 4.4:</b> Calculated absorbed dose rates ( $\text{nGyh}^{-1}$ ) of the soil and rock samples from Tabaka soapstone quarries.....	63
<b>Table 4.5:</b> Comparison of absorbed dose rates in Tabaka soapstone quarries with other areas of the world.....	66
<b>Table 4.6:</b> Comparison of calculated average absorbed dose rates and measured dose rates.....	67
<b>Table 4.7:</b> External and Internal hazard indices.....	68

**Table 4.8:** Annual effective dose rates due to extraction of soapstone at Tabaka

quarries.....69

## LIST OF FIGURES

<b>Figure 1.1:</b> Percentage contribution of ionizing radiation to humans by various sources.....	2
<b>Figure 2.1:</b> Illustration of a decay scheme of $^{226}\text{Ra}$ .....	25
<b>Figure 2.2:</b> The relative dominance of the photon interaction processes in matter.....	27
<b>Figure 2.3:</b> Illustration of the photoelectric absorption process.....	29
<b>Figure 2.4:</b> Illustration of the Compton effect.....	31
<b>Figure 2.5:</b> Illustration of the pair production process.....	32
<b>Figure 2.6:</b> Illustration of germanium detectors in liquid nitrogen dewars.....	43
<b>Figure 3.1:</b> The occurrence of Kisii Soapstone in Tabaka area.....	47
<b>Figure 3.2:</b> Block diagram illustrating gamma-ray detection system.....	51
<b>Figure 4.1:</b> Typical gamma-ray spectrum of a soil sample measured using HPGe detector.....	58
<b>Figure 4.2:</b> Figure 4.2: Comparison the mean absorbed dose rate for each quarry to the world average absorbed dose rate.....	64
<b>Figure 4.3:</b> The percentage contributions to the total absorbed dose rates due to $^{232}\text{Th}$ and $^{226}\text{Ra}$ decay products and $^{40}\text{K}$ for rock and soil samples	

from Tabaka soapstone quarries.....65

## LIST OF PLATES

<b>Plate 3.1:</b> Four selected quarries.....	48
<b>Plate 3.2:</b> The order of preparation of the rock and soil samples.....	50
<b>Plate 3.3:</b> Model 2000 Canberra radiagem that was used to measure absorbed dose rates in air.....	55

## LIST OF APPENDICES

<b>Appendix A1:</b> Thorium series.....	84
<b>Appendix A2:</b> The uranium series.....	85
<b>Appendix A3:</b> Nuclide identification reports table.....	86

## LIST OF ABBREVIATIONS AND ACRONYMS

<b>CSI</b>	Container Security Initiative
<b>CT</b>	Computer Tomography
<b>DNA</b>	Deoxyribonucleic acid
<b>EURATOM EC</b>	European Atomic Energy Community
<b>eV</b>	Electron volt
<b>HBRA</b>	High Background Radiation Areas
<b>HPGe</b>	Hyper Pure Germanium
<b>HLNRAs</b>	High Level Natural Radiation Areas
<b>IAEA</b>	International Atomic Energy Agency
<b>ICRP</b>	International Commission on Radiological Protection
<b>keV</b>	Kilo electron volt
<b>Linacs</b>	Linear Accelerators
<b>MAD</b>	Maximum Annual Effective Dose
<b>MeV</b>	Mega electron volt
<b>NaI(Tl)</b>	Sodium Iodide Thallium Activated Detector
<b>NORE</b>	Naturally Occurring Radioactive Elements
<b>rad</b>	Radiation absorbed dose
<b>REE</b>	Rare Earth Elements
<b>rem</b>	Roentgen equivalent in mammals
<b>TENORE</b>	Technologically Enhanced Naturally Occurring Radioactive Elements

<b>TLD</b>	Thermoluminescent Dosimeter
<b>UNSCEAR</b>	United Nations Scientific Committee on the Effects of Atomic Radiation
<b>Bqkg<sup>-1</sup></b>	Becquerel per kilogram
<b>SvGy<sup>-1</sup></b>	Sieverts per gray
<b>mSvy<sup>-1</sup></b>	Milli sievert per year
<b>nGyh<sup>-1</sup></b>	Nano gray per hour
<b>μgg<sup>-1</sup></b>	Micro gram per gram
<b>μSvy<sup>-1</sup></b>	Micro sievert per year
<b>Ac</b>	Actinium
<b>Bi</b>	Bismuth
<b>Cd</b>	Cadmium
<b>Co</b>	Cobalt
<b>Cs</b>	Cesium
<b>Cu</b>	Copper
<b>Fe</b>	Iron
<b>K</b>	Potassium
<b>Mn</b>	Manganese
<b>Na</b>	Sodium
<b>Pa</b>	Protactinium
<b>Pb</b>	Lead
<b>Po</b>	Polonium

<b>Ra</b>	Radium
<b>Rb</b>	Rubidium
<b>Rn</b>	Radon
<b>Th</b>	Thorium
<b>U</b>	Uranium
<b>Zn</b>	Zinc
<b>M<sub>e</sub></b>	Electronic mass
<b>H<sub>ex</sub></b>	External hazard index
<b>H<sub>in</sub></b>	Internal hazard index

## LIST OF SYMBOLS

$\alpha$	Alpha particle
$\beta$	Beta particle
$\gamma$	Gamma ray
$\lambda$	Wavelength
$\varepsilon$	Epsilon (Efficiency)
$\sigma$	Conversion coefficient
$\theta$	Scattering angle
$h$	Planck's constant
$c$	Speed of light in a vacuum

## ABSTRACT

A radiological study was carried out in the soapstone quarries of Tabaka region of Kisii district in the Southern Nyanza province, Kenya, where soapstone is mined and used as a carving medium. In this study, 14 soil and rock samples collected from five quarries were analyzed using high-resolution gamma-ray spectroscopy. The absorbed dose rates were measured 1 metre above the ground at each quarry using a model 2000 Canberra radiagem. Various radionuclides were identified in the samples. The activity concentrations of radionuclides  $^{232}\text{Th}$ ,  $^{40}\text{K}$  and  $^{226}\text{Ra}$  in the samples as well as other radiological parameters were determined. The activity concentrations for  $^{232}\text{Th}$  ranged from 38.60 to 271.70  $\text{Bqkg}^{-1}$ ,  $^{226}\text{Ra}$  ranged from 43.10 to 360.00  $\text{Bqkg}^{-1}$  and  $^{40}\text{K}$  ranged from 245.00 to 1780.00  $\text{Bqkg}^{-1}$ . The average absorbed dose rate for the five quarries measured 1 metre above the ground was 541.40  $\text{nGyh}^{-1}$ . The calculated absorbed dose rates were found to be in the range of 87.49 to 356.77  $\text{nGyh}^{-1}$ , with an overall average value of 183.79  $\text{nGyh}^{-1}$  which was 4 times higher than the world average (43  $\text{nGyh}^{-1}$ ). The corresponding annual effective dose rates due to the radionuclides  $^{232}\text{Th}$ ,  $^{226}\text{Ra}$  and  $^{40}\text{K}$  in the quarries ranged from 0.22 to 0.88  $\text{mSvy}^{-1}$ , with a mean of 0.44  $\text{mSvy}^{-1}$ , assuming a 40% occupancy factor. Both the internal and external hazard indices were found to be more than unity (1.02 and 1.28 respectively), hence exceeding the permissible limits set by International Commission on Radiological Protection, 2000. The annual effective dose in the quarries was less than 1  $\text{mSvy}^{-1}$ , the limit acceptable for the public.



## CHAPTER ONE

### 1.0 INTRODUCTION AND LITERATURE REVIEW

#### 1.1 INTRODUCTION

Human beings have always been exposed to ionizing radiations of natural origin, namely terrestrial and extra-terrestrial radiation. Extra-terrestrial exposure results from high energy cosmic ray particles while terrestrial exposure is due to the presence of naturally occurring radionuclides, mainly  $^{40}\text{K}$ ,  $^{87}\text{Rb}$ ,  $^7\text{Be}$ ,  $^{210}\text{Pb}$  and the radionuclides in the decay chains of  $^{232}\text{Th}$  and  $^{238}\text{U}$  found in soils, rocks, building materials, air, water, foodstuffs etc. The natural radioactivity in geological materials, mainly rocks and soil, come from  $^{232}\text{Th}$  and  $^{238}\text{U}$  series and natural  $^{40}\text{K}$ . Artificial radionuclides such as  $^{137}\text{Cs}$  which result from weapon testing and the Chernobyl nuclear accident can also be present (UNSCEAR, 2000). Fear of radioactivity is focused on artificial radiation sources, especially from nuclear facilities. The greatest exposure to the population is caused by natural radiation sources as shown in Figure 1.1.

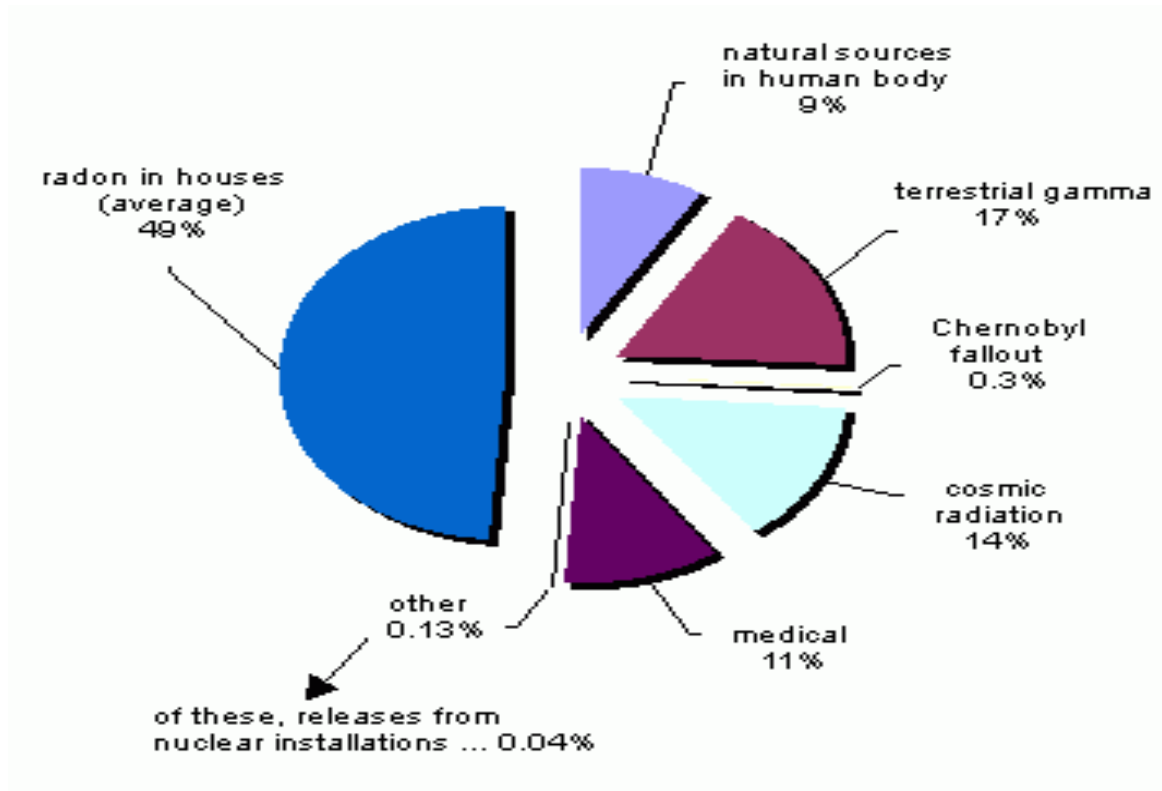


Figure1.1: Percentage contribution of ionizing radiation to humans by various sources [UNSCEAR, 2000].

The growing worldwide interest in natural radiation exposure has led to extensive surveys in many countries. To evaluate the terrestrial gamma dose rate for outdoor occupation, it is important to estimate the natural radioactivity levels in various samples. The natural radioactivity of soil samples is usually determined from the  $^{226}\text{Ra}$ ,  $^{232}\text{Th}$  and  $^{40}\text{K}$  contents (NCRP, 1993). Naturally occurring radioactive elements (NORE) including uranium and thorium are found in traces in almost all types of rocks, soil, sands and waters. NORE mineral deposits can be found in geological environments as metamorphic rocks such as gneiss, quartzfeldspathic and enderbites with interlaid mafic

horizons. From UNSCEAR (2000) reports, the greatest contribution to human exposure comes from natural background radiation, and the worldwide average annual effective dose is 2.4mSv.

## **1.2 LITERATURE REVIEW**

### **1.2.1 Earlier Studies on Terrestrial Radionuclides**

98.5% of the radiological effects of the uranium series are produced by radium and its daughter products. Extensive surveys have been carried out to determine the radium equivalent activity of soil samples in many countries (Singh *et al.*, 2003; Ibrahim., 1999; Ibrahiem *et al.*, 1993; Xinwei, 2005). Radiological studies have been made in sand beach locations, mainly in India, because along its coastline there are quite a few monazite sand bearing placer deposits causing natural high background radiation areas in Kerala and Tamilnadu, in Kalpakam and in the coast of Orissa.

The activity concentrations of  $^{226}\text{Ra}$ ,  $^{232}\text{Th}$  and  $^{40}\text{K}$  in collected soil samples have been estimated mainly by gamma ray spectrometry, although the fission track registration technique has also been used for the analysis of uranium concentration in these samples (Singha *et al.*, 2005). They found the absorbed dose rates in air, calculated the gamma dose rate from the concentration of radio-nuclides of  $^{226}\text{Ra}$ ,  $^{232}\text{Th}$  and  $^{40}\text{K}$  hence deduced the annual effective dose the inhabitants receive.

Radon ( $^{222}\text{Rn}$ ), a decay product of radium ( $^{226}\text{Ra}$ ) in the naturally occurring uranium series, is an inert gas and can diffuse through the soil, rocks and building materials. The half-life of  $^{222}\text{Rn}$  (3.8 days) is long enough for much of the radon formed in building materials or in the ground within approximately a meter of building understructures to reach the indoor environment (Mujahid *et al.*, 2005). It decays into a series of short-lived daughter products, out of which  $^{218}\text{Po}$  and  $^{214}\text{Po}$  emit high energy  $\alpha$ -particles. Radon and its progeny, when inhaled during breathing, enter the human lungs and may lead to serious diseases such as lung cancer. Since radon is a health hazard many indoor national surveys in temperate countries such as Austria, France, Russia and United States of America have been carried out to determine the level of radon and its progeny in the dwellings (Ansoborlo *et al.*, 2002, UNSCEAR; 2000). Similar studies have also been carried out in some tropical countries such as Egypt, Mexico, Latin America, Brazil, Bangladesh and Hong-Kong (Canoba *et al.*, 2001). In India many researchers are engaged in measurement of indoor radon levels in dwellings for health risk assessment and its control (Singh *et al.*, 2003).

Uranium and radium present in the soil, rocks and building materials are the main sources of indoor radon. This has brought about the need for estimation of uranium and radium content along with the radon exhalation rate in the soil (Singha *et al.*, 2005). Singha also reported that the annual effective dose in the study area varied from 1.63 to 3.45 mSv with a mean value of 2.62 mSv. Survey results have proved useful to mappers and mineral explorers and have led to additional surveys in subsequent years when new

knowledge is acquired (McCall, 1958; Patel, 1991). Anthropomorphic enhancements of the NORE, e.g. due to discharges from phosphoric factories, increases  $^{226}\text{Ra}$  activity concentrations in sediments. Although activity concentrations of  $^{226}\text{Ra}$  in environmental and geological samples are usually determined by  $\alpha$ - or  $\gamma$ - spectrometry, these methods have some drawbacks, mainly due to time and sample sizes, and hence  $\beta$ - spectrometry complements  $\alpha$ - or  $\gamma$ - spectrometry when short time is required and small samples have to be analyzed.

Studies in Canada, the United States of America, Sweden and Great Britain have shown that the ground concentration of uranium determined using an airborne gamma-ray spectrometer provides a qualitative, first-order approximation of regional variation in indoor radon levels and can be used to identify and outline high risk areas (Jackson 1992; Akerblom 1995).

In Kenya, McCall (1958) analyzed radioactive iron stone from parts of Kenya but did not report viable deposits of radioactive mineral. Mangala (1987) performed elemental analysis of sediment samples from Mrima hills and found high concentration of thorium and rare earth metals. Patel (1991) in follow up studies established that the area is composed of weathered carbonatite rock. Otwoma and Mustapha (1998) tested drinking water and building materials from soils and rock samples across seven provinces in Kenya and established presence of elevated levels of radioactivity. Against a background of growing concern over the health risk associated with exposure to natural sources of radiation, Mustapha *et al.*, (1997) analyzed the activity concentrations of

major radionuclides in some natural building materials, different types of rock and soil samples in Kenya using a gamma-ray spectrometer. The external gamma ray absorbed doses in indoor air, and the corresponding effective dose equivalents in a typical dwelling were presented. Exposures to various components of natural background radiation in Kenya were estimated using measured activity concentrations of natural radionuclides and conversion factors. Contributions to the effective dose included: 0.1 to 0.2 mSvy<sup>-1</sup> from terrestrial gamma radiation; 0.2 to 0.7 mSvy<sup>-1</sup> and a per capita of 0.4 mSvy<sup>-1</sup> from cosmic radiation; and 0.4 to 6.0 mSvy<sup>-1</sup> from inhalation of radon. Radon concentrations ranged from 5 to 1200 Bqm<sup>-3</sup> in indoor air and from 1 to 410 Bql<sup>-1</sup> in drinking water. At Buru hill carbonatite, east of Kisumu, Japanese exploration companies have prospected for rare earth elements (REE). Among such, Ohde (2004) used instrumental neutron activation analysis to determine twenty eight elements including REE from samples of carbonatite rocks from Homa mountain.

Terrestrial natural sources of radiations vary greatly from place to place. Around the world though, there are some areas with sizable populations that have high background radiation levels. The highest are found primarily in Brazil, India and China (Canoba *et al.*, 2001). The higher radiation levels are due to high concentrations of radioactive minerals in soil. One such mineral, Monazite, is a highly water insoluble rare earth mineral that occurs in beach sand. The principal radionuclides in monazite are from the <sup>232</sup>Th series, but there is also some uranium and its progeny, <sup>226</sup>Ra.

In Brazil, the monazite sand deposits are found along certain beaches. The external radiation levels on these black sands range up to  $50 \mu\text{Gyh}^{-1}$ , which is almost 400 times normal background in the US. Some of the major streets of the surrounding cities have radiation levels as high as  $1.3 \mu\text{Gyh}^{-1}$ . Another high background area in Brazil is due to deposits of large rare earth ore that form a hill that rises about 250 meters above the surrounding area. An ore near the top of the hill is very near the surface, and contains an estimated 30,000 tons of thorium and 100,000 tons of rare earth elements (Viegaa *et al.*, 2006). The radiation levels near the top of the hill are 0.01 to  $0.02 \text{ mGyh}^{-1}$  over an area of about  $30,000 \text{ m}^2$ . The plants found there have absorbed so much  $^{228}\text{Ra}$ , that they can produce a self "x-ray" if placed on a sheet of photographic paper (Srivastava *et al.*, 2002). On the Southwest coast of India, the monazite deposits are larger than those in Brazil. The dose from external radiation is on average similar to the doses reported in Brazil,  $5\text{-}6 \text{ mGyy}^{-1}$ , but individual doses up to  $32.6 \text{ mGyy}^{-1}$  have been reported. An area in China, has dose rates that are about  $3\text{-}4 \text{ mGyy}^{-1}$ . This is also from monazite that contains thorium, uranium and radium.

Achola (2009) carried out a radiological survey in various parts of Lambwe east location (South western Kenya) whose results indicated that the mean estimated annual external effective dose rate due to radionuclides in the rocks and soil was  $5704.78 \mu\text{Svy}^{-1}$ . The average specific activity concentrations of potassium-40, Radium-226 (uranium-238 equivalent) and thorium-232 in rock and soil samples from these areas were measured using gamma-ray spectrometry and found to be  $508.67 \text{ BqKg}^{-1}$ ,  $178.69 \text{ BqKg}^{-1}$  and  $1396.85 \text{ BqKg}^{-1}$  respectively. The study indicated that the source of

enhanced level of natural radioactivity in the sample was mainly carbonatite rocks. Based on the higher levels of gamma-absorbed dose rates in air ( $5.705 \text{ mSvy}^{-1}$ ) as compared to the global mean of  $0.46 \text{ mSvy}^{-1}$ , this region was considered as high natural background radiation area (HBRA) (Achola, 2009). Similar results were reported in other parts of Kenya such as Mrima hill (Mangala, 1987; Patel, 1991; Mustapha, 1999), Ruri hills, Rangwa ring complex, Soklo point and Kuge (Tuinge), in Gwasi, Suba district. (McCall, 1958; Mangala, 1987) conducted a multi-elemental X-ray fluorescence analysis of soil and rock samples from the Mrima hills. Thorium, lead, strontium and zinc were found to be at high concentration in the soil and rock samples. Thorium traces of rare earth metals were also found in high concentrations ( $>1000 \mu\text{gg}^{-1}$ ) (Mangala, 1987). Testing of Water samples from some public wells in Mrima showed radon activity levels to be around  $100 \text{ kBqm}^{-3}$  (Mustapha, 1999). This was attributed to occurrences of thorium enriched carbonates in the area.

In areas of high natural background radiation, an increased frequency of chromosome aberrations has been noted repeatedly (Achola, 2009). The increases are consistent with those seen in radiation workers and in persons exposed to high dose levels, although the magnitudes of the increases are somewhat higher than predicted. No increase in the frequency of cancer is documented in populations residing in areas of high natural background radiation (Kurnaz *et al* 2007).

Mining activities are known for their deleterious effects on the environment due to deposition of large amounts of wastes on the soil. These negative effects on the

environment caused by mining activities are mainly due to presence of high volumes of tailings. These tailings which include acidity (Wong, 1998), high concentrations of heavy toxic metals (Norland and Veith, 1995), low water retention capacity (Henriques and Fernandes, 1991) and low levels of plant nutrients (Wong, 2003) usually have unfavorable conditions to natural vegetation growing. All these factors make mine tailings sources of pollution to surface waters and soil in their vicinity (Conesa *et al.*, 2006).

A study of heavy metal concentration in growth bands of corals showed higher levels of Cu, Zn, Mn and Fe derived from mine tailings in Merinduque Island (David, 2003). Heavy metal toxicity assessment using biotest in south Morocco showed very high heavy metal concentration with Zn concentration (38,000-10,800 mgKg<sup>-1</sup>), Pb (20,412-30,000 mgKg<sup>-1</sup>), Cu (2,019-8,635 mgKg<sup>-1</sup>) and Cd (148-228 mgKg<sup>-1</sup>). The soil pH values also had wide variations (2.6-8.8), (Boularbah, 2006). A study on distribution of heavy metals from mine wastes from an old Pb-Zn mine in Spain showed very high concentrations of metal ions: 28,453.50 mgKg<sup>-1</sup> for Pb; 7,000.44 mgKg<sup>-1</sup> for Zn; 20.87 mgKg<sup>-1</sup> for Cd and 308.48 mgKg<sup>-1</sup> for Cu. High concentrations of Pb, Zn and Cd were found in many of the samples taken from surrounding arable and pasture land, indicating a certain extent of spreading of heavy metal pollution.

The existence of high-level natural radiation areas (HLNRAs) is attributed to the availability of certain radioactive minerals or elements embedded in the continental rock systems of these areas (Achola, 2009). All mineral ores contain radionuclides of natural

terrestrial origin commonly referred to as primordial radionuclides. The activity concentrations of radionuclides in normal rocks and soils are variable but generally low. However, some commercially exploited minerals contain high levels of radionuclides (Odumo, 2009).

Work activities associated with extraction, processing and use of minerals have the potential to increase exposure to radiation to members of the general public and workers. This is due to the enhanced levels of the natural radionuclides in the processed ore, depending on the type of the industrial process used in the milling of the main ore and the presence of some radionuclides associated to the main ore. This is the so called Technologically Enhanced Naturally Occurring Radioactive Elements (TENORE). Zircon is a mineral that is widely used in the ceramic industry. A radiological study on a Zircon milling plant showed total effective dose rates that were nearly the maximum acceptable value of  $1 \text{ mSvy}^{-1}$  for the members of public. Due to this the authors recommended careful monitoring and control of the industry (Ballesteros *et al.*, 2008).

Ilmenite and amang have also been assessed for their radioactive materials content. A radiological impact assessment on effects on the environment in an amang processing plant at Dengkil and Selengor, Malaysia on doses received by the public as well as occupational doses was done with the assumption that the area would be converted to a residential or industrial region once the plant was closed. The predicted maximum annual effective dose rates for residents and industrial workers were  $1.94 \text{ mSvy}^{-1}$  and  $35.00 \text{ mSvy}^{-1}$  respectively. Each of them exceeded the maximum acceptable values

(Azlina *et al.*, 2003). The activity concentration of  $^{238}\text{U}$  and  $^{232}\text{Th}$  in soils and mineral sands from the Nigerian tin mine of Bisichi area located in Jos plateau and from two control areas in Nigeria (Jos city and Akure) were done using HpGe detector. The activity concentrations in Bisichi ranged from 8.7 kBqKg<sup>-1</sup> to 51.0 kBqKg<sup>-1</sup> and 16.8 kBqKg<sup>-1</sup> to 98.0 kBqKg<sup>-1</sup> for  $^{238}\text{U}$  and  $^{232}\text{Th}$  respectively. These values were significantly high as compared to the results from the control areas and even exceeding concentrations reported for areas of high natural radioactive background. The radionuclide concentrations in foodstuffs and water in samples collected from Bisichi were found to exceed the UNSCEAR, reference values.

Funtua and Elegba (2005) estimated the radiological impact of the processing of cassiterite and Columbite from different mills of Jos Plateau (central Nigeria). The results indicated that the average dose rate at different processing points and locations at the mills had values ranging from 5  $\mu\text{Svh}^{-1}$  for the background in the premises to 80  $\mu\text{Svh}^{-1}$  for that of processed zircon. Assuming a 2,000 hours working year, workers in the processing mills were exposed to an annual dose of about 10 mSv for the background and an average of 160 mSv for processed zircon, far above the 20 mSv annual dose limit. The dose rates of about 25  $\mu\text{Svh}^{-1}$  measured for the tailings gave an annual dose of about 50 mSv for a non radiation worker in the vicinity of the milling plant, exceeding the 1 mSv<sup>-1</sup> dose limit for the members of the public. (Funtua and Elegba, 2005).

In Egyptian pyramids and tombs in the Saggara area, measurements of  $^{222}\text{Rn}$  and its progeny, as well as  $^{232}\text{Th}$  progeny were made and the results used in calculation of the maximum annual effective dose (MAD) and other important occupational radiation exposure variables. It was found that for the limited time to which occupational workers and visitors were exposed, their respective MAD values were lower than those accepted by the Regulatory Agency (i.e., 20 mSv per year for occupational workers and 1 mSv in a year for the public). However, it was shown that if the exposure times for occupational workers at three archaeological sites were to increase to normal working schedules their MAD would be exceeded. Implementation of improved ventilation practices was recommended in those sites to reduce the exposure to occupational workers (Bigu *et al.*, 2000).

Mbuzukongira, (2006) analyzed coltan samples from Congo using Gamma-ray spectrometry for activity concentration of  $^{226}\text{Ra}$  and  $^{232}\text{Th}$  in each coltan ore sample. In most of the samples  $^{40}\text{K}$  was below detection limit of the gamma spectrometer, which was calculated to be  $0.141 \text{ Bqg}^{-1}$  considering a counting time of 20 hours (72,000 seconds). All the coltan samples contained activity concentrations of  $^{226}\text{Ra}$  and  $^{232}\text{Th}$  (i.e average activity concentration ranging from 0.32 to  $1.56 \text{ Bqg}^{-1}$  for  $^{232}\text{Th}$  and 3.87 to  $13.45 \text{ Bqg}^{-1}$  for  $^{226}\text{Ra}$ ) that were much higher than the normal concentrations found in typical soil and rock samples ( $0.01$  to  $0.05 \text{ Bqg}^{-1}$  for  $^{226}\text{Ra}$  and  $0.007$  to  $0.05 \text{ Bqg}^{-1}$  for  $^{232}\text{Th}$ ). Effective dose from digging and the total dose to miners who dig coltan were calculated (Mbuzukongira, 2006). The calculated values varied widely

(from 0.007 to 18.1 mSvy<sup>-1</sup>) depending on the work activity performed by the artisans, but crushing and sieving coltan in the mills resulted in the highest dose.

The level of radiation exposure to which an average individual in the population is subjected is estimated by assuming the effective doses from all the relevant exposure pathways. Some of the inputs in the exposure assessments depend on living habits of people, e.g rate of water consumption, and fraction of time spent indoors (occupancy factor). Such inputs are estimated from available records or from experience through observations. Other inputs, either that could not be easily estimated or that do present spatial variability, are adopted from recommendations of the United Nations Scientific Committee on the Effects of Atomic Radiation (UNSCEAR) and International Commission on Radiological Protection (ICRP). Examples of the latter include the fraction of radionuclide intake that gets into the blood stream and the quality factors of different types of radiation. Doses from external exposures to cosmic radiation have been estimated from measured and calculated ionization density and neutron flux density. Shamos *et al.*, (1966) measured ionization density of cosmic rays at sea level to be 2.18 ion pairs per second per cm<sup>3</sup>, while Lodwer and Beck (1966) obtained 2.1 ion pairs per second per cm<sup>3</sup>. O'Brien used specially designed computer codes and obtained 2.16 ion pairs per second per cm<sup>3</sup>. UNSCEAR adopted 2.1 ion pairs per second per cm<sup>3</sup> and assuming a mean energy per ion pair formation in air of 33.7 eV, estimated the annual effective dose in air at sea level to be 0.24 mSv.

Biehl *et al.*, (1998) studied the effects of geomagnetic latitudes on the total cosmic ray found that the ratio of latitude effects at low geomagnetic latitudes to those at higher latitudes is roughly 65:100. Spatial variations of cosmic rays with altitude and latitude have also been reported in the works of and Merker *et al.*, (1973). The annual effective dose due to neutron component at sea level was estimated to be 0.021 mSv (UNSCEAR Report; 1998). This value was arrived at by adopting a neutron flux density at sea level of  $0.008 \text{ cm}^{-2}\text{s}^{-1}$ , a conversion factor for the neutron flux density to the dose rate of  $5 \times 10^{-8} \text{ Gyh}^{-1}\text{cm}^2$ , and a quality factor of 6 for neutrons. The neutron component was reviewed to 0.036 mSv (UNSCEAR Report; 1998) in accordance with changes in the radiation weighting factor of neutron.

Doses received from external exposure to terrestrial gamma-rays have been estimated using different techniques. Some of the earliest in-situ measurements include the use of gross gamma-ray counting and use of gamma-ray spectrometry by Lowder *et al.*, (1966). Solon *et al.*, (1980) measured the same quantity with thermoluminescent dosimeters (TLD).

In order to estimate internal dose caused by intake of a particular radionuclide, the level and distribution of the activity in the body (body burden) must be known. One of the methods that have been used to determine body burden of gamma emitters is in vitro whole-body gamma-ray counting or spectrometry. Levels and distribution of radionuclides in the body have also been determined in vitro by assaying samples of organs; tissues; body wastes like urine, faeces and breath; and environmental materials like food, water and air (Mustapha A.O 1999). Internal doses estimated from

concentrations of radionuclides in materials have some inherent limitation. The accuracy depends on the preliminary efforts made to ensure that the materials being monitored are the only route of intake of the radionuclide concerned.

### **1.2.2 Soapstone**

Soapstone is a metamorphic rock largely composed of the mineral talc and is rich in magnesium. It is produced by dynamothermal metamorphism and metasomatism which occurs at areas where tectonic plates are subducted, changing rocks by heat and pressure, with influx of fluids but without melting. The rock may feel soapy when touched, hence the name soapstone. Soapstone has been a medium for carving for thousands of years (Wikipedia.org/wiki/soapstone. 2009).

Soapstone is mined in Kenya at the Tabaka hills of Kisii district in South western Kenya. The district is mostly hilly and is dissected by rivers flowing west into lake Victoria. Most of the mining is done by men. These men are paid per kilogram of rock that is removed. The stone is mined using hoes, pangas, pick axes, shovels and iron rods. The men essentially dig pits of approximately 5 m to 30 m deep and diameter 50 m to 75 m into the ground to excavate the soapstone. No machinery is used. Once excavated, the pits are refilled by manual labour so that new soapstone begins to form and can again be excavated after 5-10 years.

Once excavated, the soapstone is mainly used in carving. Its softness makes it ideal for this purpose. Carving is done using chisels and hand tools such as hoes and knives. After curving the product is polished using sand papers of different grades to achieve a smooth surface that is ready to be painted and dyed. The coloring and dyeing is usually done by women. The porous nature of the stone allows it to easily accept dyes and colors. The product is then incised with the patterns that the individual artists wish to obtain.

### **1.3 GEOLOGY OF TABAKA REGION**

Tabaka soapstone quarries are located along Itumbe ridge and also on Sameta hill, some ten kilometers south-east of Itumbe. On the north side of Sameta hill, the white soapstone grades upwards through pale slaty-grey to dark blue-grey or almost black material at the base of the quartzite where it is slabby, with a fair development of white mica on the parting planes. In the coarse-grained quartzite immediately overlying the soapstone deposit near Kamagambo on the Kamagambo-Machoge road, there is an intense development of small pyrite cubes, up to 6mm across. In the same locality, the basalts bounding the soapstone laterally appear to have been almost completely replaced by red oxides of iron. On the North side of Itumbe hill, the white soapstone grades upwards through pale gray to dark blue material at the base of the quartzite. The normal soapstone is white and often iron stained particularly along irregular cracks and joint planes, and is soft, dense and extremely fine grained. Certain types have a pale greenish tinge.

Generally the area under investigation is characterized by a rugged topography due to the presence of several mountains of different elevation above sea level. The younger granites represent the highest elevation while the older rocks are relatively low. Climatically the area receives a good amount of rain well distributed throughout the year. It has fertile soils which the locals have put into subsistence farming (Huddleston, A 1951).

#### **1.4 PROBLEM STATEMENT**

Mining has always been associated with the exposure of radionuclides and heavy toxic elements contained in the mineral ores to the surface of the earth due to disposal of a large amount of tailings (Dudka and Adriano, 1997). At Tabaka soapstone quarries, the mined rock may expose radionuclides and heavy toxic elements. This could expose soapstone quarry workers to health effects caused by terrestrial ionizing radiation sources in the rocks. There is therefore a need to carry out a radiological study at the quarries.

#### **1.5 OBJECTIVES**

##### **1.5.1 Main Objective**

The main objective was to investigate naturally occurring radioactive elements and exposure levels to ionizing radiation at the Tabaka soapstone quarries in Kisii district of Kenya.

### **1.5.2 Specific Objectives**

The specific objectives were to:

1. determine the levels of naturally occurring radio-nuclides ( $^{40}\text{K}$ ,  $^{226}\text{Ra}$  and  $^{232}\text{Th}$ ) and their activity concentrations in soapstone quarries of Tabaka in Kisii district.
2. measure the absorbed dose rate in air at the Tabaka quarries.
3. determine the absorbed dose in air and the effective dose rate to workers at the soapstone quarries.
4. determine the internal and external hazard indices.

### **1.6 JUSTIFICATION**

No research has been done on the presence and distribution of radionuclides in Tabaka soapstone quarries. The results of this research are expected to form a data bank for exposure levels to the quarry workers and to the public within the vicinity of the soapstone quarries. This will generate a baseline database for future researchers in naturally occurring radioactive elements. It will also provide useful information for national and local authorities for decision making. This will boost the ongoing collection of relevant data required for setting up local radiological standards, guidelines and if need be legal notices. The study will also shed light on the health implications of chronic exposures to high background radiation by the soapstone artisans and inhabitants of quarry neighbourhoods.

## CHAPTER TWO

### 2.0 NATURAL RADIOACTIVITY

#### 2.1 THEORY OF NATURAL RADIOACTIVITY

Radionuclides are found naturally in air, water and soil. Every day, we ingest and inhale radionuclides in air, food and water. Natural radioactivity is common in the rocks and soil that make up the planet, in water and oceans, and in building materials. There is nowhere on earth that natural radioactivity cannot be found (Al-Sulait, *et al.*, 2008). Radioactive elements are often called radioactive isotopes or radionuclides or just radionuclides. There are over 1,500 different radioactive nuclides. The most commonly encountered radionuclides are  $^{238}\text{U}$ ,  $^{235}\text{U}$ , and their subsequent decay products and  $^{40}\text{K}$  (Matiullah, *et al.*, 2004; Ahmad, *et al.*, 1997).

Human activities such as mining, medical diagnostic and therapeutic procedures, mineral processing, nuclear power generation etc, may lead to increased exposure to naturally occurring radioactive elements called Technologically Enhanced Naturally Occurring Radioactive Elements (TENORE) (Juhašz *et al.*, 2005). TENORE is defined as exposures to truly natural sources of radiation which could not occur without some technological activities not originally designed to produce radiation. These activities have led to a large number of workers being exposed to ionizing radiations. According to (UNSCEAR, 2008) report, about 22.8 million workers are exposed to ionizing radiation with about 13 million being exposed to natural sources and about 9.8 million to

artificial sources. However due to the rapid increase in human activities this number is tremendously increasing.

International guidelines and directives for dealing with exposure due to naturally occurring radioactive elements exist though only a few countries have adopted them and made regulations for the acceptable limits of exposure for workers and the general public (ICRP, 2000; NCRP, 1993). The European Atomic Energy Community (EURATOM, 2002) and International Atomic Energy Agency (IAEA, 2004) also recommended exemption levels in activity concentrations for substances containing NORM. Based on the risk factors the ICRP has published recommendations for dose limits for the general public. For the general public, the acceptable annual effective dose limit is 1mSv per year (ICRP, 2000).

The other natural components of background radiation include cosmic rays and radiation from cosmogenic radionuclides. Cosmic radiation is divided into two types, primary and secondary. Primary cosmic radiation is made up of extremely high energy particles (above  $10^{18}$  eV), and are mostly protons, with some larger particles. A large percentage of it comes from outside of the solar system and is found throughout space. Some of the primary cosmic radiation is from the sun, produced during solar flares. Little of the primary cosmic radiation penetrates the earth's surface, the vast majority of it interacts with the atmosphere. When it does interact, it produces the secondary cosmic radiation that gets to the earth. These reactions produce other lower energy radiations in the form

of photons, electrons and neutrons that make it to the earth's surface. The atmosphere and the earth's magnetic fields act as shields against cosmic radiation, reducing the amount that reaches the earth's surface.

The annual dose received from cosmic radiation depends partly on latitude and altitude. The latitude effect is due to the charged particle nature of the primary cosmic rays. When the primary cosmic rays come near the earth, its magnetic field tends to deflect the rays away from the equator and lower latitudes and the deflection reduces toward the poles (UNSCEAR, 2000; Rasolonjatovo *et al.*, 2002). For example at latitudes lower than  $48^{\circ} 51' 29''$  North or South of the equator, the average external dose from cosmic radiation is  $305 \mu\text{Svy}^{-1}$  and approximately greater than  $350 \mu\text{Svy}^{-1}$  at latitudes higher than  $48^{\circ} 51' 29''$  North and South of the equator. The average values also increase from  $340 \mu\text{Svy}^{-1}$  at sea level to  $460 \mu\text{Svy}^{-1}$  at 1000 m above sea level (UNSCEAR, 2000; Rasolonjatovo *et al.*, 2002). From cosmic radiation in the U.S, the average person will receive a dose of 27 mrem per year and this roughly doubles every 2,000 m increase in elevation. There is only about a 10% decrease at sea level in cosmic radiation rates when going from pole to the equator, but at 18,000 m the decrease is 75%. This is because of the effect of the earth's and the Sun's geomagnetic fields on the primary cosmic radiations. Flying can add a few extra mrem to the annual dose, depending on the frequency, duration and height of flying.

Terrestrial radionuclides, are believed to have been produced when matter of which the universe is formed came into existence several billion years ago (Cox, 1995). The earth then, probably contained a large number of radioactive elements than they are at present.

The short-lived radioactive elements decayed leaving only those with half-lives comparable to the estimated age of the earth (4.6 billion years) (AGI/NAGT, 1990). The most important of these are  $^{40}\text{K}$  (half-life =  $1.28 \times 10^9\text{y}$ ),  $^{87}\text{Rb}$  (half-life =  $4.7 \times 10^{10}\text{y}$ ),  $^{232}\text{Th}$  (half-life =  $1.41 \times 10^{10}\text{y}$ ) and  $^{238}\text{U}$  (half-life =  $4.47 \times 10^9\text{y}$ ). The terrestrial component of the natural background radiation is dependent on the composition of soils and rock which typically contain natural radionuclides. Determination of soil radioactivity is essential for understanding changes in the natural radiation background (Tzortzis *et al.*, 2004). Soil generally contains small quantities of the radioactive elements, uranium and thorium along with their progeny. Primordial radionuclides of external radiation are  $^{238}\text{U}$  and  $^{232}\text{Th}$  series and  $^{40}\text{K}$ . Although  $^{235}\text{U}$  exists in soils, it accounts for very small quantities in the human body.

## **2.2 RADIOACTIVE EMISSIONS**

During radioactive decay, three ionizing radiations namely alpha particles, beta particles and gamma rays are emitted. An alpha particle is essentially a helium nucleus, which consists of two neutrons and two protons, giving it a net positive charge. Due to its relatively high mass, alpha particles are the most destructive form of ionizing radiation, but penetration is low. A piece of paper stops alpha particles, whereas the lighter beta particles require an aluminum barrier. Alpha particles are emitted from various radioactive substances. Because alpha particles have such low penetrating force, they are stopped by human skin, presenting little danger unless the source is swallowed. Other known alpha emitters include americium, radium, radon gas, and uranium. When

coupled together with certain other radioactive substances, alpha emitters can agitate neutron emitters to release the neutrons. Neutron emission is a critical part of nuclear reactor and nuclear weapons design.

The beta particle is a high-speed electron or positron released from a degenerating radioactive nucleus. Beta particles are caused by emission of excess neutrons in the atomic nucleus. When there are significantly more neutrons than protons in a nucleus, the neutrons degenerate into protons and electrons, which are ejected from the nucleus at high speeds. This increases the atomic number of the atom and also its stability. Beta emitters include strontium-90, potassium-40, technetium-99, tritium, and carbon-14. Beta particles have equivalent properties to electrons, but much higher energies than typical electrons orbiting the nucleus. Though beta particles are not themselves radioactive, they cause damage by breaking chemical bonds and creating ions which do damage to tissues. Being of medium-energy and low mass, beta particles are one of the least damaging forms of radiation. Like other radioactive substances, beta particle emitters are used in radioisotope thermoelectric generators, used to power space probes.

Gamma rays (denoted as  $\gamma$ ) are electromagnetic radiation of high frequency. Gamma-rays have the smallest wavelengths and the most energy of any other wave in the electromagnetic spectrum. They are produced by sub-atomic particle interactions such as electron-positron annihilation, neutral pion decay, radioactive decay, fusion, fission or inverse Compton scattering in astrophysical processes. Gamma rays typically have frequencies above  $10^{19}$  Hz, and therefore have energies above 100 keV and wavelength

less than 10 picometers, often smaller than an atom. Gamma radioactive decay photons commonly have energies of a few hundred keV, and are almost always less than 10 MeV in energy. Because they are a form of ionizing radiation, gamma rays can cause serious damage when absorbed by living tissue and, are therefore a health hazard.

In the past, the distinction between X-rays and gamma rays was based on energy (or equivalently frequency or wavelength), the latter being considered a higher-energy version of the former. However, high-energy X-rays produced by linear accelerators ("linacs") and astrophysical processes now often have higher energy than gamma rays produced by radioactive gamma decay. In fact, one of the most common gamma-ray emitting isotopes used in nuclear medicine, technetium-99m, produces gamma radiation of about the same energy (140 KeV) as produced by a diagnostic X-ray machine, and significantly lower energy than the therapeutic treatment X-rays produced by linac machines in cancer radiotherapy. Because of this overlap in energy ranges, the two types of electromagnetic radiation are now usually defined by their origin: X-rays are emitted by orbital electrons, while gamma rays are specifically emitted by the nucleus (that is, produced by gamma decay). In certain fields such as astronomy, gamma rays and X-rays are still sometimes defined by energy, as the processes which produce them may be uncertain (Frank, H. 2004).

### 2.2.1 Gamma Ray Production

Gamma rays are often produced alongside other forms of radiation such as alpha or beta particles. When a nucleus emits an  $\alpha$ -particle or  $\beta$ -particle, the daughter nucleus is sometimes left in an excited state. It can then jump down to a lower energy state by emitting a gamma ray as illustrated in Figure 2.1, in much the same way that an atomic electron can jump to a lower energy state by emitting infrared, visible, or ultraviolet light.

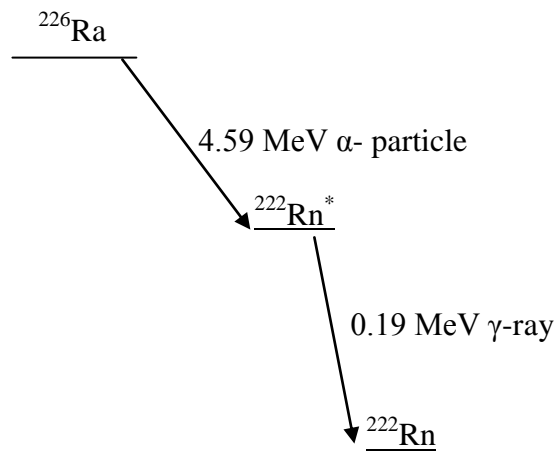


Figure 2.1 Illustration of a decay scheme of  $^{226}\text{Ra}$

Gamma rays, x-rays, visible light, and radio waves are all forms of electromagnetic radiation. The difference is the frequency and hence the energy of the photons. Gamma rays are the most energetic.

### **2.2.2 Units of Measurement and Exposure**

Measurement of gamma rays' ionizing ability is called the exposure. The effects of gamma rays and other ionizing radiation on living tissue are more closely related to the amount of energy deposited. This is called the absorbed dose.

The gray (Gy), which has units of (J/kg), is the SI unit of absorbed dose, and is the amount of radiation required to deposit 1 joule of energy in 1 kilogram of any kind of matter. The rad is the corresponding traditional unit (obsolete), equal to 0.01 J deposited per kg.  $100 \text{ rad} = 1 \text{ Gy}$ .

The equivalent dose is the measure of the biological effect of radiation on human tissue. For gamma rays it is equal to the absorbed dose. The sievert (Sv) is the SI unit of equivalent dose, which for gamma rays is numerically equal to the gray (Gy). The rem is the traditional unit of equivalent dose. For gamma rays it is equal to the rad or 0.01 J of energy deposited per kg.  $1 \text{ Sv} = 100 \text{ rem}$ .

### **2.2.3 Interaction of Gamma Rays with Matter**

Detection of gamma rays cannot occur until they interact with matter. There are several mechanisms by which gamma rays interact with matter. However, only three of these processes play an important role in radiation measurement and dosimetry: photoelectric absorption, Compton or inelastic scattering and pair production. All these result to either partial or complete transfer of the photon energy to electron energy leading to either complete disappearance of the gamma ray or it is scattered through a significant angle

(Knoll, 1988). Figure 2.2 shows the relative dominance of the photon interaction processes in matter.

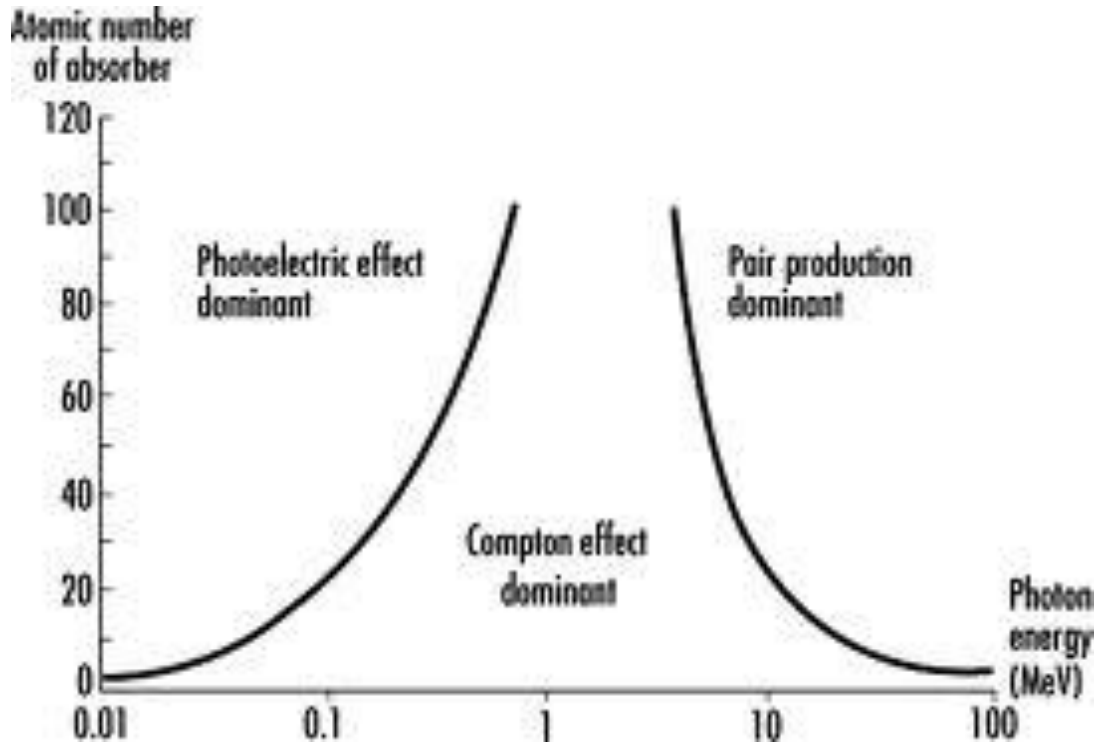


Figure 2.2: The relative dominance of the photon interaction processes in matter  
(Frank, H. 2004).

When a gamma ray passes through matter, the probability for absorption in a thin layer is proportional to the thickness of that layer. This leads to an exponential decrease of intensity with thickness. The exponential absorption holds only for a narrow beam of gamma rays. If a wide beam of gamma rays passes through a thick slab of concrete the scattering from the sides reduces the absorption.

$$I(d) = I_0 \cdot e^{-\mu d}. \quad (1)$$

Here  $\mu = n\sigma$  is the absorption coefficient, measured in  $\text{cm}^{-1}$ ,  $n$  the number of atoms per  $\text{cm}^3$  in the material,  $\sigma$  the absorption cross section in  $\text{cm}^2$  and  $d$  the thickness of material in cm.

### **2.2.3.1 Photoelectric Absorption**

When a surface is exposed to electromagnetic radiation above a certain threshold frequency (typically visible light for alkali metals, near ultraviolet for other metals, and extreme ultraviolet for non-metals), the radiation is absorbed and electrons are emitted. Photoelectric absorption takes place with photons with energies from about a few electron volts to over 1 MeV.

A gamma ray may interact with a bound electron in such a way that it loses all its energy to the target electron and the electron is ejected from the atom as illustrated in Figure 2.3.

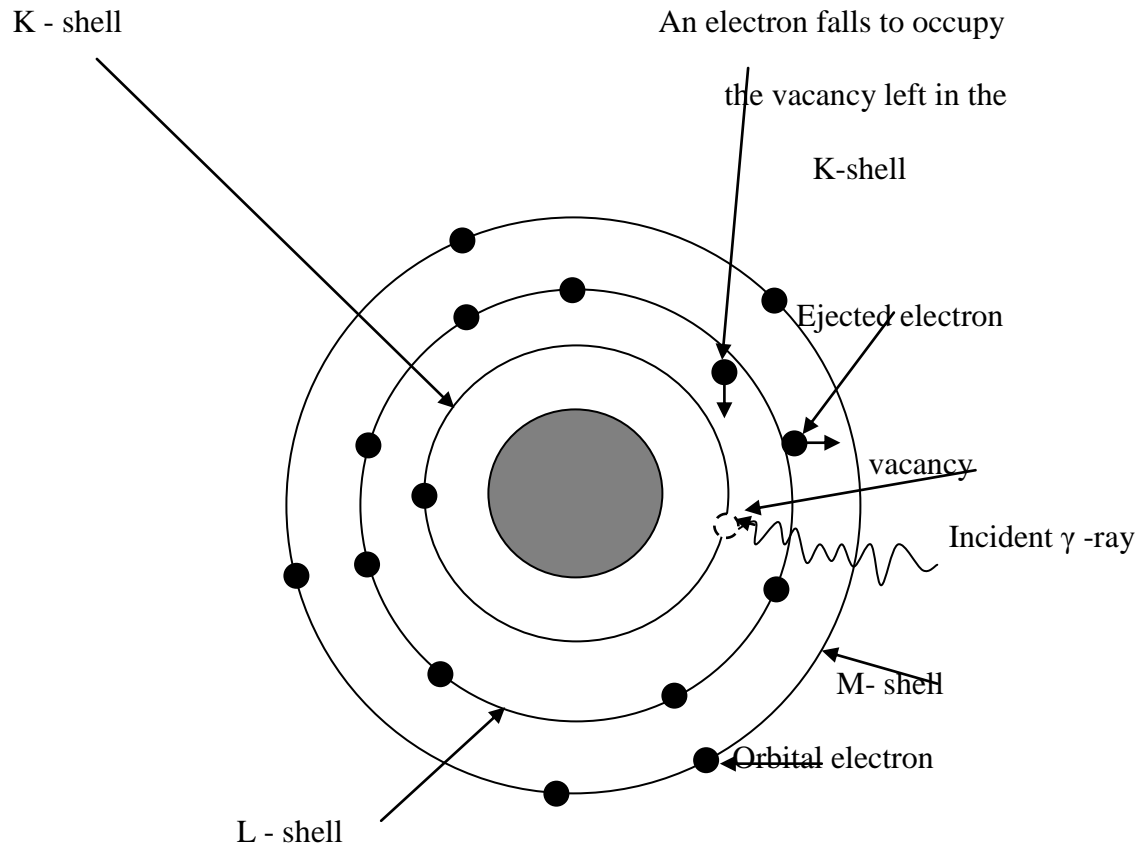


Figure 2.3: Illustration of the photoelectric absorption process

Some of the energy is used to overcome the electron binding energy and most of the remainder appear as kinetic energy of the ejected electron. A very small amount of recoil energy remains with the atom to conserve momentum. The probability of photoelectric absorption taking place depends on the gamma-ray energy, the electron binding energy and the atomic number of the atom. This probability is greater for most tightly bound

electrons. Therefore the K electrons are the most affected. The probability of photoelectric absorption is given by equation (Malace, A., *et al.*, 1996)

$$\tau = \frac{Z^4}{E^3} \quad (2)$$

The energy of the electron released by the interaction is the difference between the gamma-ray energy E and the electron binding energy E<sub>0</sub>.

$$\Delta E = E - E_0 \quad (3)$$

The electron binding energy is not lost but appears as the characteristic x-rays emitted in coincidence with the photoelectron. In most cases, these x-rays are absorbed in the detector in coincidence with the photoelectron and the resulting output pulse is proportional to the total energy of the incident gamma-ray.

### **2.2.3.2 Compton Scattering**

Compton scattering is a type of scattering that x-rays and gamma-rays undergo in matter. The scattering of photons in matter results in a decrease in energy (increase in wavelength) of an x-ray or gamma-ray photon. This effect is called the Compton effect. Part of the energy of the x-or gamma- ray is transferred to a scattering electron, which recoils and is ejected from its atom, and the rest of the energy is taken by the scattered, photon.

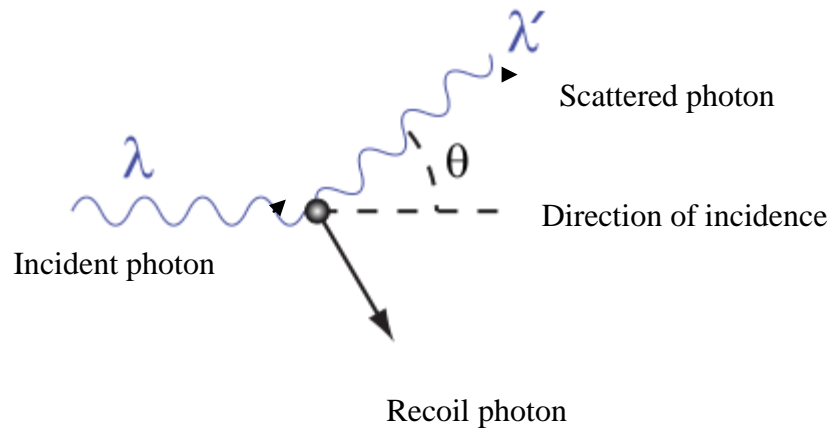


Figure 2.4: Illustration of the Compton effect

A photon of wavelength  $\lambda$  comes in from the left, collides with a target at rest, and a scattered photon of wavelength  $\lambda'$  emerges at an angle  $\theta$  (Fig 2.4).

Compton derived the relationship between the shift in wavelength and the scattering angle:

$$\lambda' - \lambda = \frac{h}{m_e c} (1 - \cos \theta), \quad (4)$$

where

$\lambda$  is the wavelength of the incident photon,

$\lambda'$  is the wavelength of scattered photon,

$h$  is the Planck constant,

$m_e$  is the mass of the electron,

$c$  is the speed of light in a vacuum, and

$\theta$  is the scattering angle.

The quantity  $h/m_e c$  is known as the Compton wavelength of the electron; it is equal to  $2.43 \times 10^{-12}$  m. The wavelength shift  $\lambda' - \lambda$  is at least zero (for  $\theta = 0^\circ$ ) and at most twice the Compton wavelength of the electron (for  $\theta = 180^\circ$ ).

Compton scattering is an important effect in gamma spectroscopy. It gives rise to the Compton edge, as it is possible for the gamma rays to scatter out of the detectors used.

### 2.2.3.3 Pair Production

Pair production refers to the creation of an elementary particle and its antiparticle usually from a photon. It occurs when a high-energy photon interacts in the vicinity of a nucleus, allowing the production of an electron and a positron pair without violating conservation of momentum as illustrated in Fig 2.5. The minimum photon energy for pair production in the vicinity of a nucleus is  $h\nu \geq 1.022 \text{ MeV}$  or twice the rest mass energy of an electron.

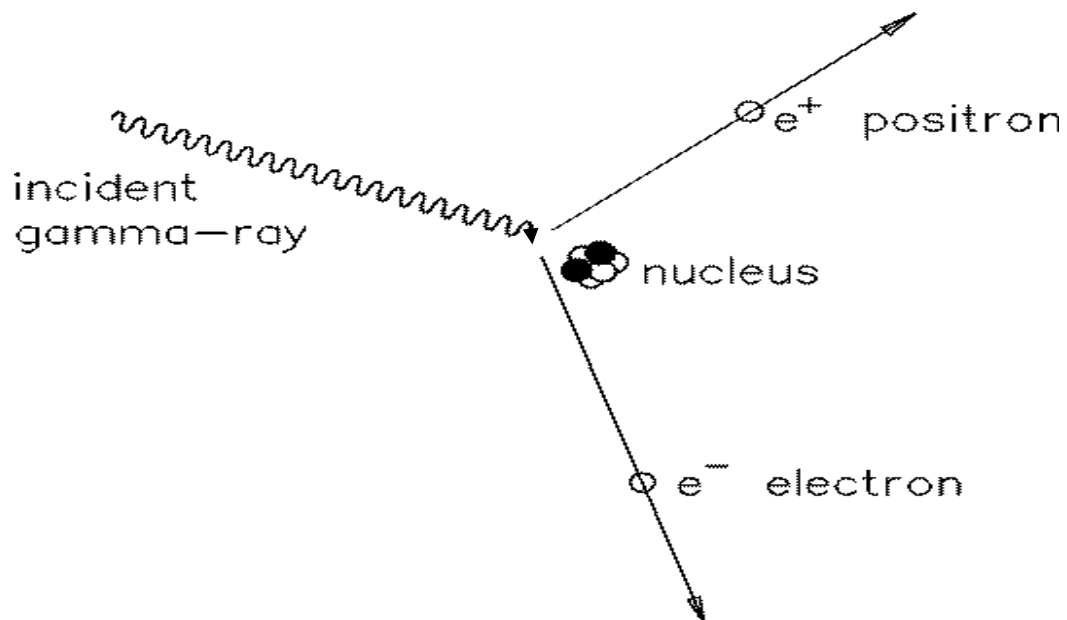


Figure 2.5: Illustration of the pair production process

## **2.3 EFFECTS OF IONIZING RADIATION ON CELLS**

The human body is made up of many organs, and each organ of the body is made up of specialized cells. Ionizing radiation can potentially affect the normal operation of these cells. Ionizing radiation absorbed by human tissue could have enough energy to remove electrons from the atoms that make up molecules of the tissue. When the electron that was shared by the two atoms to form a molecular bond is dislodged by ionizing radiation, the bond is broken and thus, the molecule falls apart. The following are possible effects of radiation on cells:

Ionization may form chemically active substances which in some cases alter the structure of the cells. These alterations may be the same as those changes that occur naturally in the cell and may have no negative effect. Some ionizing events produce substances that are not normally found in the cell. These can lead to a breakdown of the cell structure and its components. Cells can repair the damage if it is small. If a damaged cell needs to perform a function before it has had time to repair itself, it will either be unable to perform the function or perform the function incorrectly or incompletely. The result may be cells that cannot perform their normal functions or that are damaging to other cells. These altered cells may be unable to reproduce themselves or may reproduce at an uncontrolled rate. Such cells can be the underlying causes of cancers. If a cell is extensively damaged by radiation, or damaged in such a way that reproduction is affected, the cell may die. Radiation damage to cells may depend on how sensitive the cells are to radiation. All cells are not equally sensitive to radiation damage. In general,

cells which divide rapidly and/or are relatively non-specialized tend to show effects at lower doses of radiation than those which are less rapidly dividing and more specialized. Examples of the more sensitive cells are those which produce blood.

Potential biological effects depend on how much and how fast a radiation dose is received. Radiation doses can be grouped into two categories, acute and chronic dose.

An acute radiation dose is defined as a large dose (10 rad or more, to the whole body) delivered during a short period of time (on the order of a few days at the most). If large enough, it may result in effects which are observable within a period of hours to weeks. Acute doses can cause a pattern of clearly identifiable symptoms (syndromes). These conditions are referred to in general as Acute Radiation Syndrome. Radiation sickness symptoms are apparent following acute doses of 100 rad and above. Acute whole body doses of above 450 rad may result in a statistical expectation that 50% of the population exposed will die within 60 days without medical attention. As in most illnesses, the specific symptoms, the therapy that a doctor might prescribe, and the prospects for recovery vary from one person to another and are generally dependent on the age and general health of the individual. Some of the effects of acute radiation dose are;

- a) Blood-forming organ (Bone marrow) syndrome occurs at doses that are more than 100 rad is characterized by damage to cells that divide at the most rapid pace such as bone marrow, the spleen and lymphatic tissue. Symptoms include internal bleeding, fatigue, bacterial infections, and fever.

- b) Gastrointestinal tract syndrome occurs at radiation doses that are above 1000 rad and is characterized by damage to cells that divide less rapidly such as the linings of the stomach and intestines. Symptoms include nausea, vomiting, diarrhea, dehydration, electrolytic imbalance, loss of digestion ability, bleeding ulcers, and the symptoms of blood-forming organ syndrome.
- c) Central nervous system syndrome occurs at radiation doses that are more than 5000 rad and is characterized by damage to cells that do not reproduce such as nerve cells. Symptoms include loss of coordination, confusion, coma, convulsions, shock, and the symptoms of the blood forming organ and gastrointestinal tract syndromes.

Other effects from an acute dose include: 200 to 300 rad to the skin can result in the reddening of the skin, similar to a mild sunburn and may result in hair loss due to damage to hair follicles.

125 to 200 rad to the ovaries can result in prolonged or permanent suppression of menstruation in about fifty percent (50%) of women. 600 rad to the ovaries or testicles can result in permanent sterilization. 50 rad to the thyroid gland can result in benign (non cancerous) tumors. As a group, the effects caused by acute doses are called deterministic. This means that severity of the effect is determined by the amount of dose received.

A chronic dose is a relatively small amount of radiation received over a long period of time. The body is better equipped to tolerate a chronic dose than an acute dose. The

body has time to repair damage because a smaller percentage of the cells need repair at any given time. The body also has time to replace dead or non-functioning cells with new, healthy cells. This is the type of dose received as occupational exposure. The biological effects of high levels of radiation exposure are fairly well known, but the effects of low levels of radiation are more difficult to determine because the deterministic effects do not occur at these levels. The risks for these effects are not directly measurable in populations of exposed workers, therefore the risk values at occupational levels are estimates based on risk factors measured at high doses. To make these estimates, a relationship between the occurrence of cancer at high doses and the potential for cancer at low doses are used. Since the probability for cancer at high doses increases with increasing dose, this relationship is assumed to hold true with low doses. This type of risk model is called stochastic.

Somatic effects appear in the exposed person while genetic effects appear in the future generations of the exposed person as a result of radiation damage to the reproductive cells. They may be divided into two classes namely prompt somatic effects and delayed somatic effects based on the rate at which the dose was received. Prompt somatic effects are those that occur soon after an acute dose (typically 10 rad or more to the whole body in a short period of time). One example of a prompt effect is the temporary hair loss which occurs about three weeks after a dose of 400 rad to the scalp. New hair may to grow within two months after the dose, although the colour and texture may be different. Delayed somatic effects are those that occur years after radiation doses are received. Among the delayed effects is an increased potential for the development of cancer.

Since a fetus is especially sensitive to radiation, (fetus cells are rapidly dividing) special considerations are given to pregnant workers particularly in the first 20 weeks of pregnancy. Limits are established to protect the fetus from any potential effects which may occur from a significant amount of radiation. This radiation exposure may be the result of exposure to external sources of radiation or internal sources of radioactive material. Potential effects associated with prenatal radiation doses include: growth retardation, small head/brain size, mental retardation and childhood cancer. At present occupation dose limits, the actual probability of any of these effects occurring in the fetus from occupational exposure of the mother is small (UNSCEAR, 2008).

### **2.3.1 Health Effects of Gamma Rays**

All ionizing radiation causes similar damage at a cellular level, but because alpha and beta rays are relatively non-penetrating, external exposure to them causes only localized damage, e.g. radiation burns to the skin. Gamma rays and neutrons are more penetrating, causing diffuse damage throughout the body (e.g. radiation sickness, increased incidence of cancer) rather than burns. External radiation exposure should also be distinguished from internal exposure, due to ingested or inhaled radioactive substances, which, depending on the substance's chemical nature, can produce both diffuse and localized internal damage. The most biological damaging forms of gamma radiation occur in the gamma ray window, between 3 and 10 MeV, with higher energy gamma rays being less harmful because the body is relatively transparent to them (Rothkamm, K 2003).

Shielding from gamma rays requires large amounts of mass. They are better absorbed by materials with high atomic numbers and high density, although neither effect is important compared to the total mass per area in the path of the gamma ray. For this reason, a lead shield is only modestly better (20-30%) as a gamma shield than an equal mass of another shielding material such as aluminum, concrete, or soil; the lead's major advantage is in its compactness.

The higher the energy of the gamma rays, the thicker the shielding required. Materials for shielding gamma rays are typically measured by the thickness required to reduce the intensity of gamma rays by one half (the half-value-layer or HVL). For example gamma rays that require 1 cm of lead to reduce their intensity by 50% will also have their intensity reduced in half by 4.1 cm of Granite rock, 6 cm of concrete, or 9 cm of packed soil. However, the mass of this much concrete or soil is only 20-30% larger than that of this amount of lead. Depleted uranium is used for shielding in portable gamma ray sources, but again the savings in weight over lead is modest, and the main effect is to reduce shielding bulk.

Gamma radiation is often used to kill living organisms, in a process called irradiation. Applications of this include sterilizing medical equipment (as an alternative to autoclaves or chemical means), removing decay-causing bacteria from many foods or preventing fruit and vegetables from sprouting to maintain freshness and flavour. Due to their tissue penetrating property, gamma rays have a wide variety of medical uses such as in CT scans and radiation therapy. However, as a form of ionizing radiation they have

the ability to effect molecular changes, giving them the potential to cause cancer when DNA is affected. The molecular changes can also be used to alter the properties of semi-precious stones, and is often used to change white topaz into blue topaz. Despite their cancer-causing properties, gamma rays are also used to treat some types of cancer. In the procedure called gamma-knife surgery, multiple concentrated beams of gamma rays are directed on the growth in order to kill the cancerous cells. The beams are aimed from different angles to concentrate the radiation on the growth while minimizing damage to the surrounding health tissues. Gamma rays are also used for diagnostic purposes in nuclear medicine. Several gamma-emitting radioisotopes are used, one of which is technetium-99m. When administered to a patient, a gamma camera can be used to form an image of the radioisotope's distribution by detecting the gamma radiation emitted from the target organs of the body. Such a technique can be employed to diagnose a wide range of conditions (e.g. spread of cancer to the bones). In the US, gamma ray detectors are used as part of the Container Security Initiative (CSI). The objective of this technique is to screen merchant ship containers before they enter US ports.

## **2.4 GAMMA RAY DETECTORS**

These detectors are either the scintillation type or the semiconductor type. In scintillation detectors, primary electrons produced by the gamma-ray interaction raise secondary electrons to the conduction band, leaving holes in the valence band. In some cases the energy given to the electron may not be quite sufficient to raise it to the conduction band. The electron will therefore fall back to the valence band emitting electromagnetic

radiation. If this radiation is in or near optical wavelengths, it can be detected by a photomultiplier or other light measuring devices to provide the detector signal. This is the basis of the scintillation detector.

A good scintillation material has a reasonable number of electron-hole pairs produced per unit gamma-ray energy, high atomic number, is transparent to the emitted light, a short decay time of the excited state to allow high count rates and a refractive index that is near that of glass (1.5) to permit efficient coupling to photomultipliers. Materials that have found particular application for gamma-ray measurements are, sodium iodide, cesium iodide, cesium fluoride and bismuth germinate. The most commonly used scintillator material is sodium iodide because it is cheap and readily available.

A semiconductor is a material whose conductivity lies between that of insulators and conductors. In an insulator, the valence band is full and the next available energy states are in a higher band called the conduction band, separated by a wide forbidden region. Electrons are not able to jump across this forbidden region hence the material cannot conduct. In a conductor, the valence and conduction bands overlap, hence electrons easily move from the valence band to the conduction band. In semiconductors, the forbidden gap is narrow. When electrons in the valence band of a semiconductor are thermally excited, they are able to jump across the forbidden region to the conduction band. This is the basis of the semiconductor gamma-ray detector.

A good semiconductor detector material has a high atomic number and provides as many electron-hole pairs as possible per unit energy. It also allows good electron and hole mobility, is available in high purity as near perfect single crystals and is available in reasonable amounts at reasonable cost. Some of the semiconductors that meet the requirements include silicon and germanium. The disadvantage of silicon over germanium is its lower atomic number, which means that in practice it is only used in measurement of low energy photons. Detectors based on silicon are in routine use in x-ray spectrometry.

Germanium is by far the most common gamma-ray detector material. Its higher atomic number than silicon makes it practicable to use for detection of higher energy gamma radiation. The germanium detector may be thought of as being like a solid ionization chamber, it has a p-n diode structure in which the intrinsic region is created by depletion of charge carriers when a reverse bias is applied across the diode. When photons interact with the depletion region, charge carriers (holes and electrons) are freed and are swept to their respective collecting electrodes by the electric field. The detector configurations ensure that an electric field is present throughout the active volume so that both charge carriers feel electrostatic forces that cause them to drift in opposite directions. The motion of either the electrons or holes constitutes a current that will persist until those carriers are collected at the boundaries of the active volume. The resultant charge is

integrated by a charge sensitive preamplifier and converted to a voltage pulse with amplitude proportional to the original photon energy.

Due to the small band gap (0.7 eV); room- temperature operation of germanium detectors of any type is impossible because of the large thermally induced leakage current that would result. Instead, germanium detectors must be cooled to reduce the leakage current to the point that associated noise does not spoil their excellent energy resolution. Normally the temperature is reduced to 77 K through the use of an insulated Dewar in which a reservoir of liquid nitrogen is kept in thermal contact with the detector as illustrated in Fig 2.6.

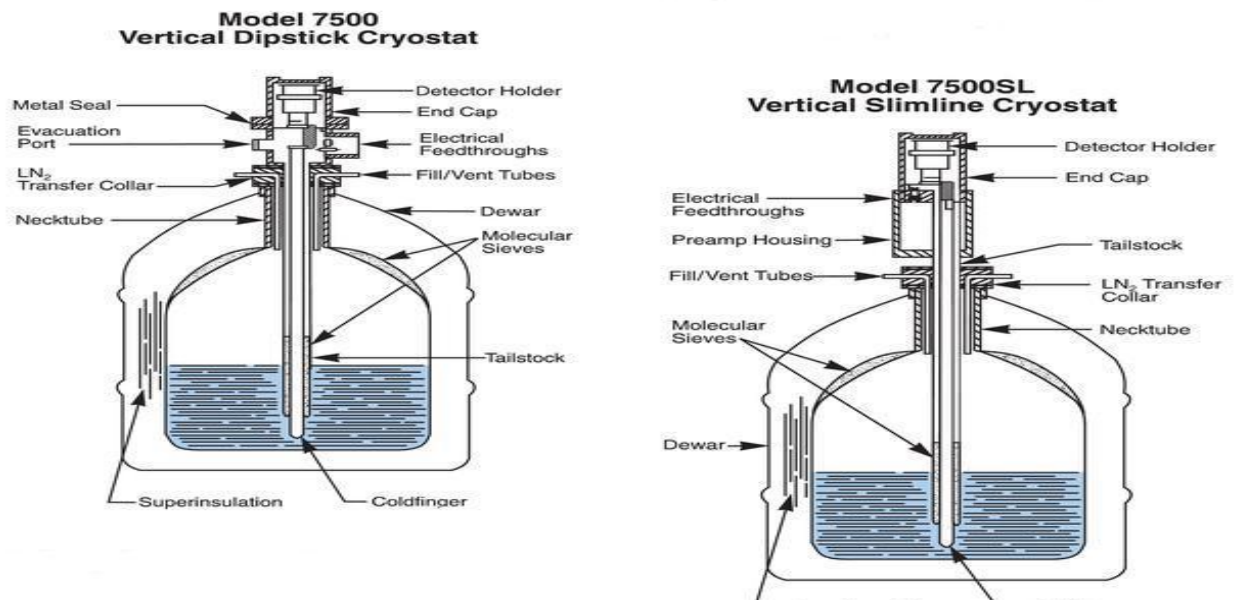


Figure 2.6: Illustration of germanium detectors in liquid nitrogen dewars (Khan H. *et al.*, 1993)

### 2.4.1 Energy Resolution

Resolution is a measure of the width (full width at half maxima) of a single energy peak at a specific energy, either expressed in absolute keV (as with germanium detectors), or as a percentage of the energy at that point (sodium iodide detectors). Better resolution enables the system to more clearly separate the peaks within a spectrum.

The dominant characteristic of germanium detectors is their excellent energy resolution when applied to gamma-ray spectroscopy. This allows the separation of many closely spaced gamma-ray energies, which remain unresolved in the NaI(Tl) spectrum. Consequently, virtually all gamma-ray spectroscopy that involves complex energy spectra is now carried out with germanium detectors. The increased number of charge carriers has two beneficial effects on the attainable energy resolution. The statistical fluctuation in the number of carriers per pulse becomes a smaller fraction of the total as the number is increased. At low energies the resolution may be limited by electronic noise.

#### **2.4.2 Detector Efficiency**

The efficiency of a detector is a measure of how many pulses occur for a given number of gamma rays. Various kinds of efficiency definitions are in common use for gamma ray detectors:

Absolute efficiency: The ratio of the number of pulses produced by the detector to the number of gamma-rays emitted by the source (in all directions). Intrinsic efficiency: The ratio of the number of pulses produced by the detector to the number of gamma-rays striking the detector.

Relative efficiency: Efficiencies of one detector relative to another. Full energy peak (photo peak) efficiency: The efficiency for producing full energy peak pulses only, rather than a pulse of any size for the gamma ray. To be useful, the detector must be capable of absorbing a large fraction of gamma ray energy.

Gamma-ray spectrometry of naturally occurring radioactive elements is difficult for a number of reasons. First, the activity levels are low and if statistically significant results are to be obtained, there is need for long count periods. The second reason is that most gamma-spectrometer devices are not able to block background counts due to radionuclides in the surroundings of the detector. Therefore the activity in the sample itself must be detected on top of all that background activity. In many cases it will be necessary to make a peaked background correction in addition to the normal continuum subtraction. Semiconductor detectors like germanium detectors that overcome the two challenges have been designed (Gordon, 2008).

## CHAPTER THREE

### 3.0 MATERIALS AND METHODS

#### 3.1 SAMPLE COLLECTION

The rock and soil samples were collected from Nyatike location, Bomanyara and Bomware sub locations of Tabaka region. At Bomanyara, samples were collected from two quarries, one owned by Samson Orege and the other by Peter Nyaberi. At Bomware samples were collected from three quarries, two named after their owners Joshua Ouma and Reuben Barongo and a third one called British quarry (Fig 3.1). Samples could not be collected at the same depths in each quarry because soapstone was not occurring at the same levels for all the quarries. A total of 14 samples were collected from the five quarries (Table 3.1).

Table 3.1: Quarry identity and sample type collected

Quarry name	Orege	Nyaberi	Ouma	Barongo	British
Sample type showing depth at which it was collected	Rock 5m	Rock 4m	Rock 8m	Rock 8m	Rock 15m
	Rock 3m	Rock 7m	Rock 4m	Rock 4m	Rock 1m
	Soil 0.3m		Soil 1m	Soil 0.3m	Soil 0.3m

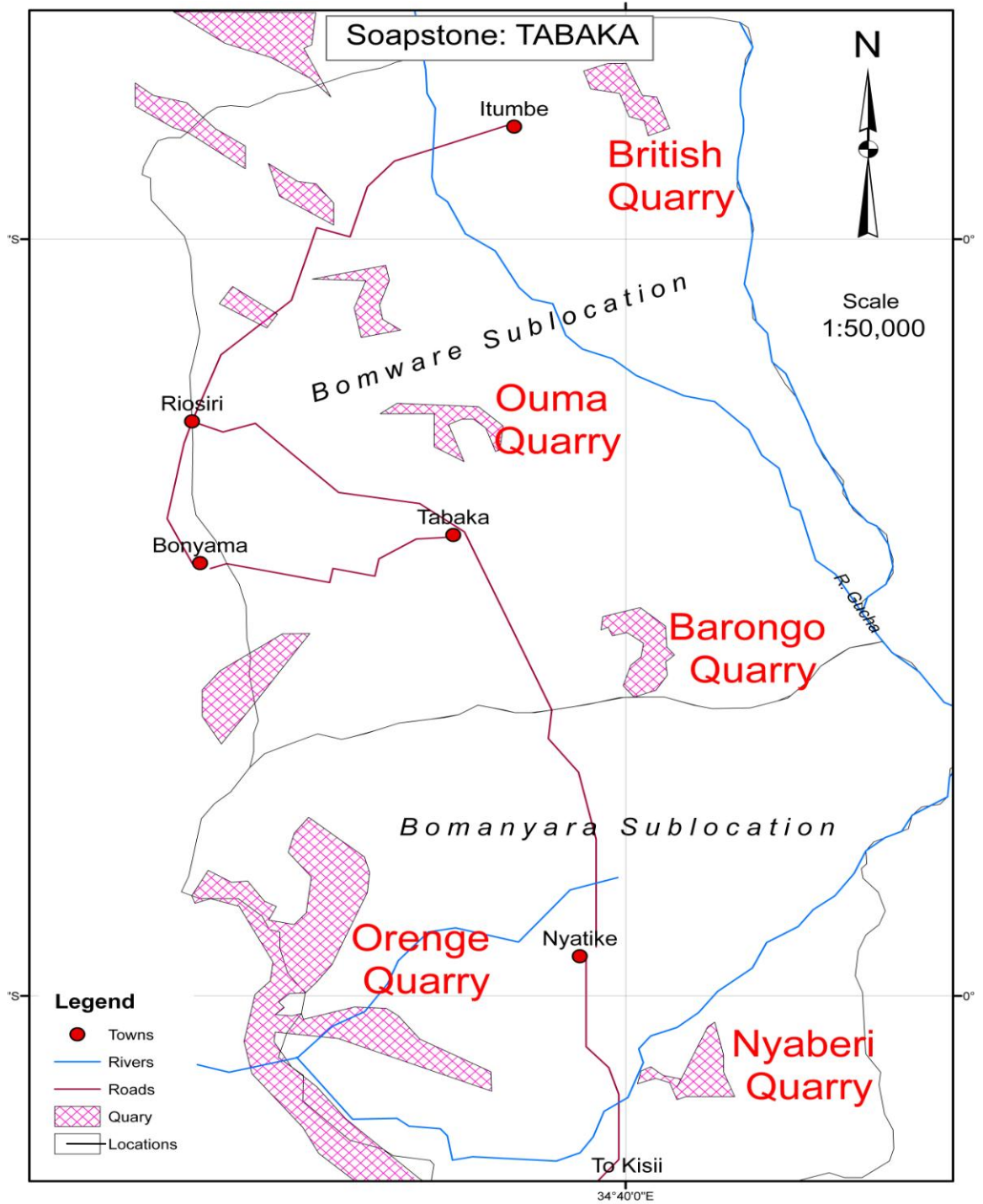


Figure 3.1: The occurrence of Kisii Soapstone in Tabaka area

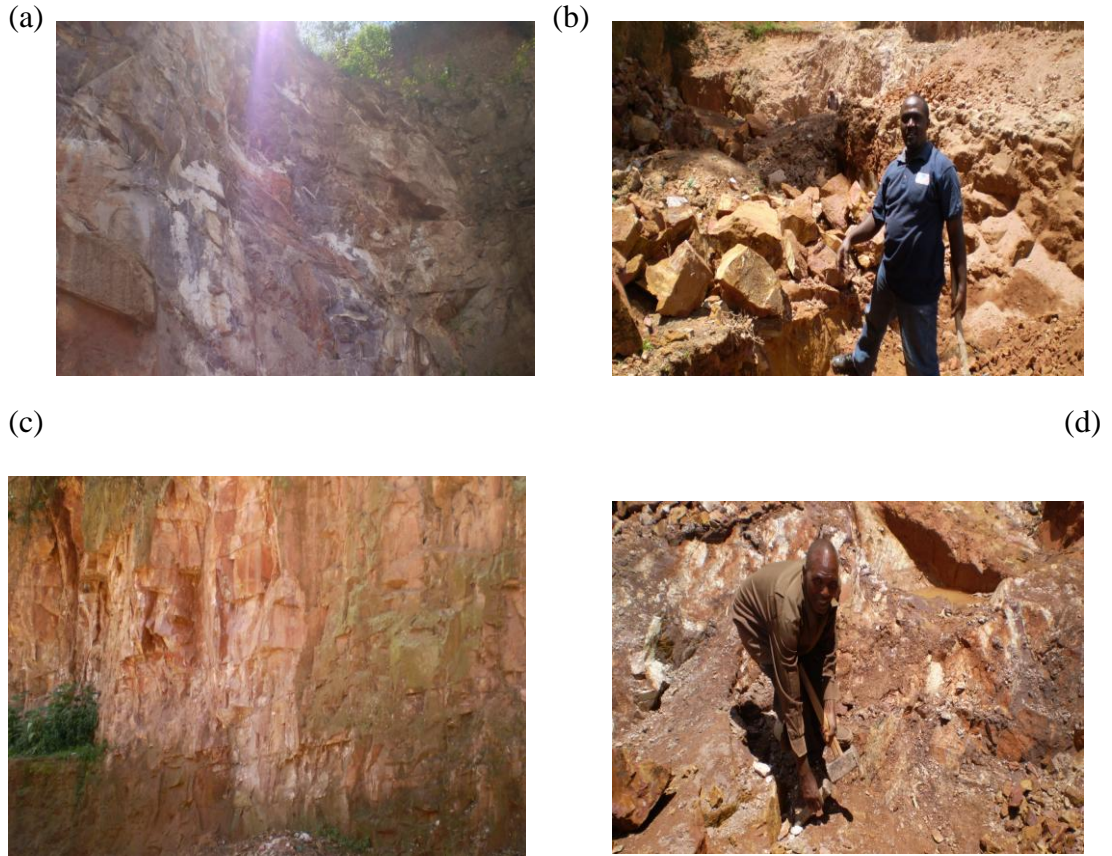


Plate 3.1: Four selected quarries showing (a) Ouma's quarry, with the Pink colour clearly showing the soapstone rock, (b) British quarry, showing a refilled section behind the worker, (c) an abandoned quarry and (d) Orange's quarry, showing the hand tools that are used to extract the rock

### **3.2 SAMPLE PREPARATION**

After collection, the rock and soil samples were separately crushed into powder form and sieved through a 0.6 mm mesh sieve. They were then dried in an oven at 80<sup>0</sup>C for 24 hours, completely removing water from the samples. A mass of 200g of each sample was packed in special gas tight polyethylene plastic containers then closed and tightly sealed using cellotape. The containers were labeled appropriately and then kept for 30 days. After this period all the decay products in the <sup>232</sup>Th series and <sup>226</sup>Ra sub-series were in radioactive equilibrium with their daughters. The samples were then taken for gamma spectrometric analysis at the National Radiation Protection Laboratory (NRPL). The order of sample preparation is shown in plate 3.2.



Plate 3.2: The steps and devices for preparation of the rock and soil samples. Shown in the figure are, (a) samples being crushed using a manual grinding machine, (b) the 0.6mm wire mesh sieve, (c) crushed samples drying in an oven, (d) samples packed in labeled polythene bags and (e) a sample placed inside a hyper pure germanium detector

### 3.3 ACTIVITY CONCENTRATION MEASUREMENTS

The concentrations of radionuclides ( $^{226}\text{Ra}$ ,  $^{232}\text{Th}$  and  $^{40}\text{K}$ ) in each sample were determined using a high purity germanium (HPGe) gamma ray spectrometer consisting of a p-type intrinsic germanium coaxial detector (ORTEC model 7450) mounted vertically. The detector had a relative efficiency of 33 % and full width at half maximum (FWHM) of 2.0 keV energy resolution for the 1332 keV gamma ray line of  $^{60}\text{Co}$ . The detector was connected to a Canberra multichannel analyzer (MCA) with apex software, that allowed data acquisition, display of gamma-spectra, analysis of the gamma-spectra and storage of the results in memory counters called channels. The MCA was interfaced with a computer and a printer (Fig 3.2). The detector was housed inside a 10 cm thick lead shield internally lined with 2 mm Cu foils. This provided an efficient suppression of background gamma radiation present within the laboratory. To ensure that all nuclides due to  $^{238}\text{U}$  and  $^{232}\text{Th}$  were visible in the gamma spectrum, spectral data acquisition time for the each sample was 12 hours.

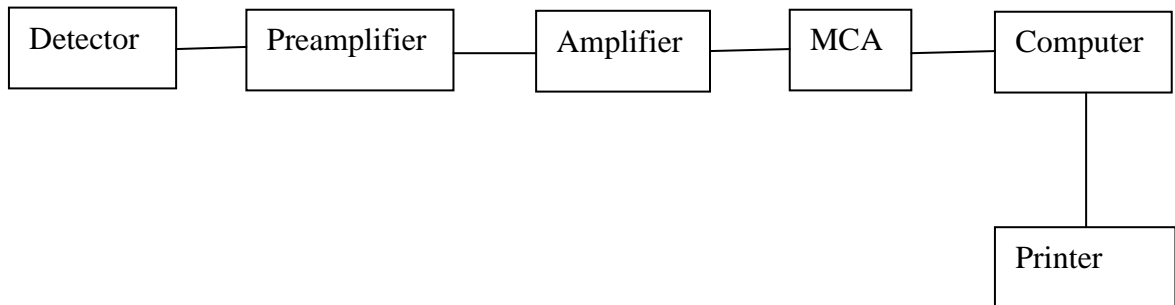


Figure 3.2: Block diagram of a gamma-ray MCA detection system

The activity concentration for each radionuclide in the measured samples was determined by the net intensity of respective peaks. Equation 5 could also be used to calculate activity concentration.

$$C_s = \frac{N_a}{\epsilon p t \omega} \text{ (BqKg}^{-1}\text{)} \quad (5)$$

Where  $C_s$  is the activity concentration,  $N_a$  is the net count for the gamma ray,  $\epsilon$  is the counting efficiency of the detector,  $P$  is the absolute transition probability for gamma decay per transformation,  $t$  is the counting time in seconds and  $\omega$  is the weight of the dried sample in kilograms. The analysis of results was performed using Microsoft Excel software.

Geometric efficiency for soil matrices was determined by a reference soil standard (International Atomic Energy Agency, IAEA-365) spiked with a series of nuclides ( $^{40}\text{K}$ ,  $^{212}\text{Bi}$ ,  $^{212}\text{Pb}$ ,  $^{214}\text{Bi}$ ,  $^{214}\text{Pb}$ ,  $^{137}\text{Cs}$ ,  $^{228}\text{Ac}$ ,  $^{234}\text{Pa}$ ,  $^{235}\text{U}$ ) with total activity of  $2.848 \text{ kBqkg}^{-1}$  as on the day 02.02.2010 at 11:32:52 am (Table 3.2).

Table 3.2: Identified radionuclides for IAEA – 365 soil sample

Nuclide name	Absolute emission probability of gamma decay (%)	Energy $\pm$ 0.005 (keV)	Activity $\pm$ 0.005 (Bqkg <sup>-1</sup> )
<sup>40</sup> K	10.67	1460.81	296.00
<sup>137</sup> Cs	85.12	661.65	2420.00
<sup>212</sup> Bi	11.80	727.17	12.10
<sup>212</sup> Pb	44.60	238.63	13.40
<sup>214</sup> Bi	46.30	609.31	11.90
<sup>214</sup> Pb	37.20	351.92	12.70
<sup>228</sup> Ac	27.70	911.60	19.50
<sup>234</sup> Pa	0.59	1001.03	57.20
<sup>235</sup> U	54.00	185.71	5.29

### 3.4 RADIONUCLIDE IDENTIFICATION REPORTS

The <sup>226</sup>Ra activities for samples assumed to be in radioactive equilibrium were estimated from <sup>214</sup>Pb (351.92 keV) and <sup>214</sup>Bi (609.31 keV). The gamma-ray energies of <sup>212</sup>Bi, <sup>212</sup>Pb and <sup>228</sup>Ac were used to estimate activity of <sup>232</sup>Th. The activity concentrations of <sup>40</sup>K were measured directly by its own gamma rays (1460.81 keV). Details of the employed spectroscopic parameters are shown in Table 3.3

Table 3.3: Spectroscopic parameters employed for quantification of activity levels

(Tsai, L, *et al.*, 2008)

Element	Emitter nuclide	Half-life of nuclide	Gamma-ray energy (keV)	Absolute emission probability of gamma decay (%)
<sup>226</sup> Ra	<sup>214</sup> Bi	19.90 min	609.31	46.30
	<sup>214</sup> Pb	26.80 min	351.92	37.20
<sup>232</sup> Th	<sup>212</sup> Bi	60.55 min	727.17	11.80
	<sup>212</sup> Pb	10.64 h	238.63	44.60
	<sup>228</sup> Ac	6.25 h	911.60	27.70
<sup>40</sup> K		$1.3 \times 10^9$ y	1460.81	10.67

### 3.5 ABSORBED DOSE

Two approaches were used to estimate the external absorbed doses that result from deposition of radionuclides in soil surfaces: direct measurements and calculations based on radionuclide deposition densities.

#### 3.5.1 Measurement of Absorbed Dose Rates In Air

Absorbed dose rates in air were measured 1m above the surface at each quarry using a hand held survey meter Canberra-radiagem 2000 model (Plate 3.3) with a reading range of up to 100  $\mu\text{Svh}^{-1}$ . Absorbed dose rates in air in  $\text{nGyh}^{-1}$  were computed from the dose rates in  $\mu\text{Svh}^{-1}$  as measured in the field using the conversion coefficient factor of 0.7  $\text{SvGy}^{-1}$  as recommended by UNSCEAR, 2000.



Plate 3.3: Model 2000 Canberra radiagem that was used for measurement of absorbed dose rates in air

### 3.5.2 Calculation of Absorbed Dose Rates

Radiation emitted by a radioactive substance is absorbed by any material it encounters. UNSCEAR (2000) has given the dose conversion factors for converting the activity concentrations of  $^{226}\text{Ra}$ ,  $^{232}\text{Th}$  and  $^{40}\text{K}$  into dose ( $\text{nGyh}^{-1}$  per  $\text{Bqkg}^{-1}$ ) as 0.427, 0.662 and 0.043, respectively. Using these factors, the total absorbed dose rate in air is calculated as given in the equation (6) (UNSCEAR 2000).

$$D = (0.427C_{\text{Ra}} + 0.662C_{\text{Th}} + 0.043C_{\text{K}}) \text{ nGyh}^{-1}, \quad (6)$$

where  $C_{\text{Ra}}$ ,  $C_{\text{Th}}$  and  $C_{\text{K}}$  are the activity concentrations ( $\text{Bqkg}^{-1}$ ) of radium, thorium and potassium in soil respectively.

### 3.5.3 Calculation of Annual Effective Dose

Effective dose is a dosimetric quantity used for comparing health effects of radiation to the human body. To estimate the annual effective dose (AED), take into account the conversion coefficient, ( $0.7 \text{ SvGy}^{-1}$ ) from the absorbed dose in air to effective dose and

the outdoor occupancy factor. The average fraction of time spent indoor and outdoor (occupancy factors) in Kenya are 0.6 and 0.4 respectively (Mustapha, 1999). The world average indoor and outdoor occupancy factors are 0.8 and 0.2 respectively (UNSCEAR, 2000).

The effective dose rate in units of  $\text{mSvy}^{-1}$  was estimated using the formula (UNSCEAR, 1998);

$$\text{Effective dose rate} = \eta \Phi \sigma (8.76 \times 10^{-6}) \quad (7)$$

where  $\sigma = 0.7 \text{ SvGy}^{-1}$  is the conversion coefficient,  $\eta$  is absorbed dose rate in  $\text{nGyh}^{-1}$  and  $\Phi = 0.4$  is the outdoor occupancy factor in Kenya.

#### 3.5.4 External Hazard Index ( $H_{ex}$ )

Radiation exposure due to  $^{226}\text{Ra}$ ,  $^{232}\text{Th}$  and  $^{40}\text{K}$  may be external. This hazard, defined in terms of external hazard index or outdoor radiation hazard index and denoted by  $H_{ex}$ , can be calculated using the equation (Beretka and Mathew 1985):

$$H_{ex} = \frac{C_{Ra}}{370} + \frac{C_{Th}}{259} + \frac{C_K}{4810} \quad (8)$$

where  $C_{Ra}$ ,  $C_{Th}$  and  $C_K$  are activity concentrations of  $^{226}\text{Ra}$ ,  $^{232}\text{Th}$  and  $^{40}\text{K}$  respectively in  $\text{Bqkg}^{-1}$ . The value of this index should be less than 1 in order for the radiation hazard to be considered acceptable to the public (Beretkab and Mathew, 1985).

### 3.5.5 Internal Hazard Index ( $H_{in}$ )

The internal hazard index ( $H_{in}$ ) gives the internal exposure to carcinogenic radon and is given by the formula (Beretkab and Mathew, 1985):

$$H_{in} = \frac{C_{Ra}}{185} + \frac{C_{Th}}{259} + \frac{C_K}{4810} \quad (9)$$

where  $C_{Ra}$ ,  $C_{Th}$  and  $C_K$  are activity concentrations of  $^{226}\text{Ra}$ ,  $^{232}\text{Th}$  and  $^{40}\text{K}$ , respectively, in  $\text{Bqkg}^{-1}$ . The value of this index should be less than unit in order for the radiation hazard to have negligible hazardous effects of radon to the respiratory organs of the public (Beretkab and Mathew, 1985).

## CHAPTER FOUR

### 4.0 RESULTS AND DISCUSSION

#### 4.1 GAMMA-RAY SPECTRUM FOR A SOIL SAMPLE

A gamma-ray spectrum of one of the soil samples that were analyzed using HPGe is shown in Figure 4.1.

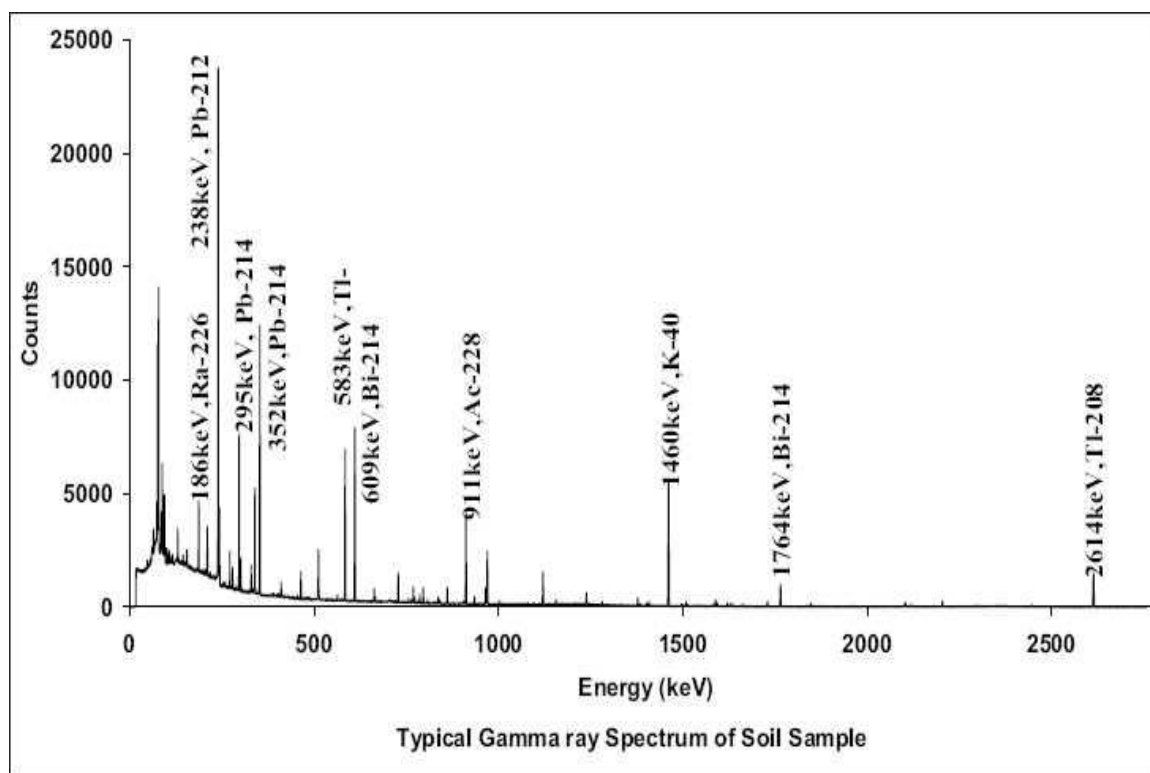


Fig 4.1: Typical gamma-ray spectrum of a soil sample measured using HPGe detector.

Based on the spectroscopic parameters employed for quantification (Table 3.3) and the gamma ray spectra for various samples (Fig 4.1), several radionuclides were identified in the soil and rock samples as shown in appendix A3.

## 4.2 ACTIVITY CONCENTRATIONS OF RADIONUCLIDES IN THE SAMPLES

Data on activity concentration of radionuclides  $^{226}\text{Ra}$ ,  $^{232}\text{Th}$  and  $^{40}\text{K}$  in rock and soil (all values reported as  $\text{Bqkg}^{-1}$ ) collected from soapstone quarries at Tabaka is given in Table 4.1.

Table 4.1: Activity of radionuclides  $^{232}\text{Th}$ ,  $^{226}\text{Ra}$  and  $^{40}\text{K}$  in the measured rock and soil samples from Tabaka soapstone quarries in Kenya

Quarry name	Depth of point of collection of sample (m)	Activity concentration ( $\text{Bqkg}^{-1}$ ) $\pm 0.005$		
		$^{232}\text{Th}$	$^{226}\text{Ra}$	$^{40}\text{K}$
Orengo	0.3	147.70	72.60	587.00
	3	84.80	43.10	1780.00
	5	38.60	52.20	922.00
Nyaberi	4	263.30	75.80	307.00
	7	100.20	52.50	1020.00
Ouma	1	120.80	49.90	887.00
	4	93.90	63.30	813.00
	8	258.40	360.00	744.00
Barongo	0.3	15.76	78.20	641.00
	4	172.15	61.00	245.00
	8	92.70	177.90	1090.00
British	0.3	210.40	72.70	534.00
	1	271.70	82.00	284.00
	15	236.50	65.80	403.00

It can be seen in Table 4.1 that the general activity of  $^{226}\text{Ra}$  and  $^{232}\text{Th}$  in the collected soil and rock samples were in the range of 43.1-360  $\text{Bqkg}^{-1}$  and 38.6-271.7  $\text{Bqkg}^{-1}$  respectively. There was no particular relationship between activity of the radionuclides and depth of the point of collection of the sample. This could be attributed to the fact that there may have been mixing of rock debris during refilling of the quarries for formation of new soapstone which is again excavated after 5-10 years.

In all quarries  $^{40}\text{K}$  had the highest activity concentration. Its activity varied widely between 245 and 1780  $\text{Bqkg}^{-1}$  due to heterogeneous soil characteristics, the lowest being at Barongo's quarry and the highest at Orange's quarry.

The variation of natural radioactivity levels at different sampling sites was due to the variation of concentrations of radionuclides in the geological formations. The younger granites represent the highest elevation while the elevation in older rock is relatively low. The presence of such high radioactivity in younger granites may be attributed to the presence of relatively increased amount of accessory minerals such as zircon, iron oxides, fluorite and other radioactive related minerals. These minerals play an important role in controlling the distribution of uranium and thorium. Zircon usually contains uranium and thorium concentration ranging from 0.01% to 0.19% and 1% to 2% respectively (Cuney *et al.*, 1987). Uranium in iron oxides is trapped by adsorption (Speer *et al.*, 1981).

A comparison between the average activity concentrations of radionuclides in each quarry and the world average activity concentrations of the respective radionuclides was done in Table 4.2. All the average values of activity concentrations of  $^{40}\text{K}$ ,  $^{226}\text{Ra}$  and

$^{232}\text{Th}$  were higher than the world wide average activity concentrations of  $^{40}\text{K}$ ,  $^{226}\text{Ra}$  and  $^{232}\text{Th}$  which are 400, 35 and 30  $\text{Bqkg}^{-1}$  respectively as reported by UNSCEAR (2000).

Table 4.2: Comparison between average activities of radionuclides in each quarry and the world average activities of the radionuclides.

Quarry name	Radionuclides	Average activity $\pm 0.05$ ( $\text{Bqkg}^{-1}$ )	World average activity $\pm 0.05$ ( $\text{Bqkg}^{-1}$ )(UNSCEAR, 2000)
Orengé	$^{232}\text{Th}$	90.3	30
	$^{226}\text{Ra}$	56.0	35
	$^{40}\text{K}$	1096.3	400
Nyaberi	$^{232}\text{Th}$	181.8	30
	$^{226}\text{Ra}$	64.2	35
	$^{40}\text{K}$	663.5	400
Ouma	$^{232}\text{Th}$	157.7	30
	$^{226}\text{Ra}$	157.7	35
	$^{40}\text{K}$	814.7	400
Barongo	$^{232}\text{Th}$	93.5	30
	$^{226}\text{Ra}$	105.7	35
	$^{40}\text{K}$	658.7	400
British	$^{232}\text{Th}$	240.0	30
	$^{226}\text{Ra}$	73.5	35
	$^{40}\text{K}$	407.0	400

### 4.3 ABSORBED DOSE RATES

#### 4.3.1 Measured Absorbed Dose Rates

The absorbed dose rates in air measured 1 m above the surface at each quarry are presented in Table 4.3. These values vary from 480 – 597 nGyh<sup>-1</sup>, the lowest dose being experienced at Nyaberi’s quarry and the highest at British quarry. The average measured absorbed dose rate for the five quarries is 541.4 nGyh<sup>-1</sup>, which is 9.2 times higher than the world average value of 60 nGyh<sup>-1</sup> (UNSCEAR, 2000).

Table 4.3: Absorbed dose rates measured 1 m above the surface at each quarry

Quarry name	Absorbed dose rates± 0.5 (nGyh <sup>-1</sup> )
Orege	483
Nyaberi	480
Ouma	557
Barongo	590
British	597

#### 4.3.2 Calculated Absorbed Dose Rates

The absorbed dose rates due to terrestrial gamma rays 1m above the ground were calculated using equation (6) and were expressed in nGyh<sup>-1</sup>. Other radionuclides such as <sup>137</sup>Cs, <sup>235</sup>U, <sup>231</sup>Th, <sup>211</sup>Bi and <sup>22</sup>Na were neglected because their contribution to the total

dose rates from environmental background is negligible (Kocher and Sjoreen, 1985).

The results of the calculations are presented in Table 4.4.

Table 4.4: Calculated absorbed dose rates ( $\text{nGyh}^{-1}$ ) of the soil and rock samples

Quarry name	Depth (in m) of point of collection of sample	Absorbed dose rate $\pm 0.005$ ( $\text{nGyh}^{-1}$ )			Total absorbed dose rate $\pm 0.005$ ( $\text{nGyh}^{-1}$ )
		$^{232}\text{Th}$	$^{226}\text{Ra}$	$^{40}\text{K}$	
Orengo	0.3	97.78	31.00	25.24	154.02
	3	56.14	18.40	76.54	151.08
	5	25.55	22.29	39.65	87.49
Nyaberi	4	174.30	32.34	13.20	219.84
	7	66.33	22.42	43.86	132.61
Ouma	1	79.97	21.31	38.14	139.42
	4	62.16	27.90	34.96	125.02
	8	171.06	153.72	31.99	356.77
Barongo	0.3	104.33	33.39	27.56	165.28
	4	113.96	26.05	10.54	150.55
	8	61.37	75.96	46.87	184.20
British	0.3	139.28	31.04	22.96	193.28
	1	179.86	35.01	12.21	227.08
	15	156.56	28.10	17.33	201.99

The calculated total absorbed dose rates due to  $^{226}\text{Ra}$ ,  $^{232}\text{Th}$  and  $^{40}\text{K}$  in rocks and soils varied between  $87.49 \text{ nGyh}^{-1}$  to  $356.77 \text{ nGyh}^{-1}$  as shown in Table 4.4. The computed average absorbed dose rates in each of the quarries were 130.9, 176.23, 207.07, 166.68 and  $207.45 \text{ nGyh}^{-1}$  for Orengé's, Nyaberi's, Ouma's, Barongo's and British quarries respectively and were all higher than the world average as illustrated in Figure 4.2. The calculated average absorbed dose rate ( $183.79 \text{ nGyh}^{-1}$ ) for the five quarries was found to be about 4.3 times higher than the world average ( $43 \text{ nGyh}^{-1}$ ) as reported by UNSCEAR (2000).

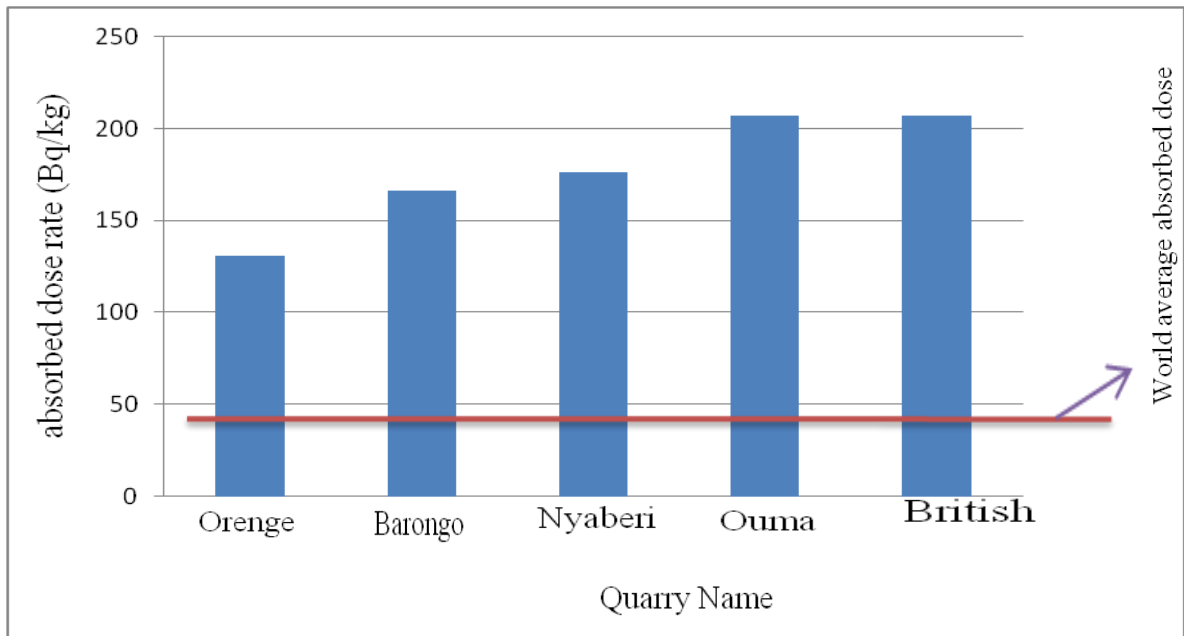


Figure 4.2: Comparison of the mean absorbed dose rate for each quarry to the world average absorbed dose rate.

The contribution by each of the radionuclides  $^{226}\text{Ra}$ ,  $^{232}\text{Th}$  and  $^{40}\text{K}$  to the total absorbed dose rate at the quarries were 25% ( $45.96 \text{ nGyh}^{-1}$ ), 58% ( $106.3 \text{ nGyh}^{-1}$ ) and 17% ( $31.5 \text{ nGyh}^{-1}$ ) respectively as illustrated in Figure 4.3.

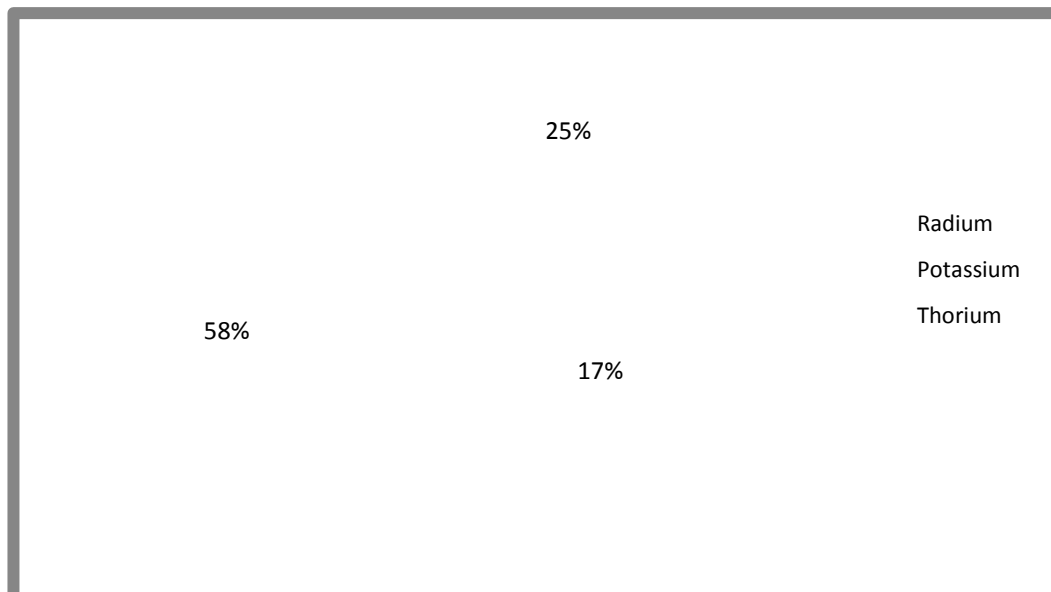


Figure 4.3: The percentage contributions to the total absorbed dose rates due to  $^{232}\text{Th}$ ,  $^{226}\text{Ra}$  decay products and  $^{40}\text{K}$  for rock and soil samples from Tabaka soapstone quarries.

A comparison between absorbed dose rates at Tabaka soapstone quarries and absorbed dose rates at other places in the world was done. Details of the comparison are presented in Table 4.5.

Table 4.5: Comparison of absorbed dose rates in Tabaka soapstone quarries with other areas of the world.

Country	Absorbed dose rates $\pm 0.5$ (nGyh <sup>-1</sup> )	References
Orisa, India	1925	Mohanty <i>et al.</i> , 2004
Ruri hill, Kenya	949	Achola, 2009
Minas, Brazil	220	Malanka <i>et al.</i> , 1993
Firtina valley, Turkey	77	Kurnaz <i>et al.</i> , 2007
Xiazhuang, China	124	Yang <i>et al.</i> , 2005
Eskisehir, Turkey	167	Orgun <i>et al.</i> , 2005
Eastern desert, Egypt	488	Arafa, 2004
Tabaka, Kenya	184	Present study

The measured and calculated absorbed dose rates were compared in Table 4.6 and it was noted that the measured absorbed dose rates in air were much higher than the calculated absorbed dose rates for all the quarries. The reason for the difference is that the measured absorbed dose rates included the dose due to cosmic rays while the calculated absorbed dose rates did not.

Table 4.6: Comparison of calculated average absorbed dose rates and measured dose rates.

Quarry name	Measured absorbed dose rates $\pm 0.5$ (nGyh <sup>-1</sup> )	Calculated average absorbed dose rates $\pm 0.5$ (nGyh <sup>-1</sup> )
Orengé	483	131
Nyaberi	480	176
Ouma	557	207
Barongo	590	167
British	597	207

#### 4.4 EXTERNAL HAZARD INDEX AND INTERNAL HAZARD INDEX

The ultimate use of the measured activities in building materials is to estimate the radiation dose expected to be delivered externally if a building is constructed using these materials. To limit the annual external gamma-ray dose to 1 mSvy<sup>-1</sup> (ICRP, 2000), the external hazard index was calculated using equation (8). Results of these calculations are presented in Table 4.7. The average external hazard index from all the samples was 1.02. This average value slightly more than unity, the acceptable average value (ICRP, 2000).

Table 4.7: External and Internal hazard indices

Quarry name	Depth (m) of point collection of sample	External hazard index ( $H_{ex}$ ) $\pm$ 0.005	Internal hazard index ( $H_{in}$ ) $\pm$ 0.005
Orege	0.3	0.89	1.08
	3	0.81	0.93
	5	0.48	0.62
Nyaberi	4	1.29	1.49
	7	0.74	0.88
Ouma	1	0.79	0.92
	4	0.70	0.87
	8	2.12	3.10
Barongo	0.3	0.95	1.16
	4	0.88	1.05
	8	1.07	1.55
British	0.3	1.12	1.32
	1	1.33	1.55
	15	1.17	1.35
Average		1.02	1.28

Internal exposure to  $^{222}\text{Rn}$  and its radioactive progeny is controlled by the internal hazard index ( $H_{in}$ ) which is given by equation (9). Calculated values of  $H_{in}$  are also presented in Table 4.7. The average internal hazard index for all the samples is 1.28. For safe use of a material in the construction of dwellings,  $H_{in}$  should be less than unity (ICRP, 2000).

#### 4.5 ANNUAL EFFECTIVE DOSE RATE

The annual effective dose rates that a quarry worker receives by extracting soapstone from the quarries are presented in Table 4.8.

Table 4.8: Annual effective dose rates due to extraction of soapstone at Tabaka quarries

Quarry name	Depth (in m) of point of collection of sample	Effective dose rate $\pm 0.0005$ (mSvy <sup>-1</sup> )
Orengé	0.3	0.378
	3	0.371
	5	0.215
Nyaberi	4	0.539
	7	0.325
Ouma	1	0.342
	4	0.305
	8	0.875
Barongo	0.3	0.403
	4	0.369
	8	0.452
British	0.3	0.474
	1	0.557
	15	0.495

The mean annual effective dose rate in all the samples is  $0.44 \text{ mSvy}^{-1}$ . The value is more than the average annual effective dose rate ( $5.62 \text{ } \mu\text{Svy}^{-1}$ ) received by artisanal gold miners at Osiri, Macalder, Mikei and Masara gold mines in South Nyanza (Odumo, 2009). The average value and all the annual effective dose rate values in Table 4.8 are less than the  $5.71 \text{ mSvy}^{-1}$  obtained by Achola 2009 in a radiological survey carried out at Lambwe east location and are also less than  $1 \text{ mSvy}^{-1}$  which is the annual effective dose rate limit for the public (ICRP, 2000). Results of effective doses from Tabaka soapstone quarries, gold mines of parts of South Nyanza and the radiological survey at Lambwe valley were compared because these places are close to each other. From the results it is noted that Lambwe valley has an effective dose that is more than the limit acceptable for the public and therefore can be considered a high background radiation area.

## CHAPTER FIVE

### 5.0 CONCLUSIONS AND RECOMMENDATIONS

#### 5.1 CONCLUSIONS

The activity concentrations of  $^{226}\text{Ra}$ ,  $^{232}\text{Th}$  and  $^{40}\text{K}$  were all found to be above the world's average. In all quarries sampled,  $^{40}\text{K}$  had the highest activity concentration. The measured average absorbed dose rate in air ( $541.4 \text{ nGyh}^{-1}$ ) at the soapstone quarries was 9 times higher than the world measured average ( $60 \text{ nGyh}^{-1}$ ) and 2.9 times higher than the calculated average.

The calculated average absorbed dose rate in air ( $183.79 \text{ nGyh}^{-1}$ ) due to gamma-ray emitters in the soapstone quarries was at least 4 times higher than the world average ( $43 \text{ nGyh}^{-1}$ ). Thorium and potassium contributed the highest and lowest values respectively to the average absorbed dose rate in the quarries. The averages for both the external (1.02) and internal (1.28) hazard indices exceeded a unity, the limit acceptable by ICRP 2000. Therefore soapstone rock obtained from Tabaka area is not suitable for construction of houses. The annual effective dose rate in the quarries ( $0.44 \text{ mSvy}^{-1}$ ) was less than  $1 \text{ mSvy}^{-1}$ , the acceptable limit for the public.

Since the annual effective dose rate obtained is less than the limit set for the public, soapstone carvings and other soapstone products pose no radiation threat to the public.

## **5.2 RECOMMENDATIONS**

Based on the results and conclusions drawn from this study, the following are recommended:-

Quarry workers should be encouraged to maintain high personal hygiene practices such as washing hands thoroughly at meal times because there is a possibility of high levels of toxic elements like lead in the mines. The gamma spectrometric analysis done in this study revealed the presence of radioactive lead in the soapstone samples.

To avoid radiological contamination, tools used in the quarries should not be mixed with tools used for other purposes such as utensils as this may increase possible exposure pathways.

- Soapstone rock obtained from Tabaka area should not be used as building material since both the internal and external hazard indices obtained were more than the acceptable limit. However, should it be used for building, adequate ventilation is recommended.
- The soil and rock samples should be collected from more quarries for analysis to get more representative results. The samples should also be collected at different times of the year since climatical changes in the year could affect dispersion of radionuclides.
- Research should be done to determine the presence of heavy metals in soapstone.
- The government should provide machinery for quarrying to the miners as this may reduce the time they spend in the quarries (occupancy factor) hence reducing the annual effective dose rate they receive.

- Clear policies on quarrying that pay closer attention to the effects of quarrying to the environment should be put in place and the government should hold the miners responsible for any environmental pollution during and after mining.

## REFERENCES

- Achola, S. O. 2009.** Radioactivity and elemental analysis of carbonites rocks from parts of Gwasi area, south western Kenya. M.Sc. Thesis, University of Nairobi.
- AGI/NAGT. 1990.** American Geological Institute and the National Association of Geology Teachers. Laboratory manual in physical Geology, second edition., Merrill Publishing Co., London. Pp 134-156.
- Akerblom, G. 1995.** “The use of Airborne Radiometric and Exploration Survey Data and techniques in radon risk mapping in Sweden”, Application of uranium exploration data and techniques in environmental studies, International Atomic Energy Agency Technical Document 827.
- Aly, A.A., Hassan, M.H. and Huwait, M.R.A. 1999.** Radioactivity assessment of fabricated phosphogypsum mixtures. Fourth Radiation Physics Conference, 15–19 November 1999, Alexandria, Egypt: Pp 632–640.
- Ansoborlo, E., Chazel, V., Henge-Napoli, M. H., Pihet, P., Rannou, A., Bailey, M.R., Stradling, N (2002).** “Determination of the physical and chemical properties, biokinetics and dose coefficients of uranium compounds handled during nuclear fuel fabrication in France”, *Health physics*. **82(3)**.
- Arafa, W., 2004.** Specific activity and hazards of granite samples collected from the eastern desert of Egypt. *Journal of environmental radioactivity*. **75**, Pp 315-327
- Beretka,J.,Mathew,P.J. 1985.** Natural radioactivity of Australian building materials, industrial wastes and by-products. *Health physics*. **48**, Pp 87-95

- Biehl, A., Neher, H., Roesch, W. (1998).** Cosmic ray experiments at high altitudes. *Health and safety laboratory*, New York Pp 914-932.
- Bigu, J., Mohamed, I. H. and Hussein, A. Z. 2000.** Radiation measurements in Egyptian pyramids and tombs-occupational exposure of workers and the public. *Journal of Environmental Radioactivity* **47**, Pp 245-252.
- Bock, R. K. 2008.** "Very-High-Energy Gamma Rays from a Distant Quasar: How Transparent Is the Universe?". *Science* **320**, Pp 1752–1754.
- Boularbah, A., Schwartz, C., Bitton, G. and Morel J. L. 2006.** Heavy metal contamination from mining sites in South Morocco: Use of a biotest to assess metal toxicity of tailings and soil. *Chemosphere* **63**, Pp 802-810.
- Canoba, A., Lopez,F.O., Arnaud, M.I., Oliveria, A.A., Neman, R.S., Hadler, J.C., Iunes, P.J., Paulo, S.R., Osorio, A.M., Aparecido, R., Rodriguez, C., Moreno, V., Vasquez, R., Espinosa, G., Golarri, J.I., Martinez, T., Navarrete, M., Cabrera, I., Sagovia, N., Pena, P., Tamez, E., Pereyra, P., Lopez, H.M.E., Sajo, B.L.,(2001)** "Indoor radon measurements and methodologies in Latin American Countries", *Radiation Measurement*, 34:
- Conesa, H. M., Faz, A. and Raquel, A. 2006.** Heavy metal accumulation and tolerance in plants from mine tailings of the semi arid Cartagena La- Union mining district (SE Spain). *Science of the total environment* **366**, Pp 1-11.
- Cox, P.A. 1995.** The elements on earth. Inorganic chemistry in the environment, Oxford university press, New York.

- Cuney, M., LeFort, P., Wangeg, Z. 1987.** Geology of Granites and their Metallogenic Relations. *Science Press*, Moscow. Pp 852-873.
- David, C. P. 2003.** Heavy metal concentration in growth bands of corals: a record of mining tailings input through time (Marinduque Island, Philippines). *Marine Pollution Bulletin* **46**, Pp 187-196.
- Department for Environment, Food and Rural Affairs (DEFRA) UK. 2003.** Key facts about radioactivity. Pp 127
- Dodson, R. G. 1953.** A geology of south east machakos area. *Geological Survey Kenya*. **25**, Pp 3
- Dudka, S. and Adriano, C. D. 1997.** Environmental impacts of metal ore mining and processing. *Journal of the Environment*. **26**, Pp 590-602.
- European Commission (EC). 2002.** Practical use of the concepts of clearance and exemption, Part II, application of the concepts of exemption and clearance of natural radiation sources. *Radiation Protection*. **122**, Pp 213-218
- Frank, H. A. 2004.** Introduction to radiological physics and radiation dosimetry. Wiley-VCH Verlag GmbH and company. KGaA, Weinheim, Germany. Pp 234-345.
- Funtua, I. I. and Elegba, S. B. 2005.** Radiation exposure from high-level radiation area and related mining and processing activities of Jos Plateau, central Nigeria. International Congress Series **1276**, Pp 401– 402.
- Gregory, R. L. 1992.** Analytical electron microscopy of Columbite: A niobium-tantalum oxide mineral with zonal uranium distribution. *Journal of Nuclear Materials* **190** North-Holland: Pp 302-311.

- Gordon, R.G. 2008.** Practical gamma-ray spectrometry. John Willey and sons Ltd. Warrington UK.
- Huddleston. A. 1951.** Geology of the Kisii district. Degree sheet 41.goverment printer, Nairobi: Pp 24.
- Karakelle, B., Ozturk, N., Kose, A., Varinlioglu, A., Erkol, A. Y and Yilmaz, F. 2002.** Natural radioactivity in soil samples of kocaeli basin, Turkey. *J. Radioanal Nuclear Chemistry.* **254**, Pp 649-651.
- Khan, H. A., Qureshi, I. E. and Tufail, M. 1993.** Passive dosimetry of Radon and its daughters using solid state nuclear track detectors (SSNTDs). *Radiation protection dosimetry*, **46**, Pp 149-170.
- Kocher, D.C., Sjoreen, A.L. 1985.** Dose-rate conversion factors for external exposure to photon emitters in soil. *Health physics.* **48**, Pp 193-205.
- Kurnaz, A., Keser, R., Okumusoglu, N.T., Karahan, G., Cevic, U. 2007.** Determination of radioactivity levels and hazards of soil and sediment samples in Firtina Valley (Turkey), *Applied Radiation and Isotopes* **65** (2007), Pp1281-1289.
- Gupta, C. K. and Suri A. K. 1994.** Extractive Metallurgy of Niobium, CRC Press, USA: Pp 21-121.
- Habashi, F. 1997.** Handbook of Extractive Metalurgy, vol. 3, Wiley-VCH, Germany: Pp1404-1421.
- Henriques, F. S. and Fernandes, J. C. 1991.** Metal uptake and distribution in rush (*Juncus Conglomeratus*) plants growing in pyrites mine tailings at Lousal, Portugal. *Total Environment.* **102**, Pp 253-260.

- International Atomic Energy Agency (IAEA). 2004.** Application of the Concepts of Exclusion, Exemption and Clearance. Safety Series No. RS-G-1.7 (Vienna: IAEA).
- Ibrahiem, N.M., Abdel-Ghani, A.H., Shawky, S.M., Ashraf, E.M. and Farouk, M.A. 1993.** Measurement of radioactivity levels in soil in the Nile Delta and Middle Egypt. *Health Physics*. **64**, Pp 620–627.
- International Commission on Radiation Protection (ICRP). 2000.** Protection of the public in situations of prolonged radiation exposure ICRP Publication 82; Ann. ICRP 29 (1–2), Pergamon Press, Oxford.
- Juhász, L., Serbin, P. and Czoch, I. 2005.** Evaluation of technologically enhanced naturally occurring radioactive materials in Hungary. International congress series. **1276**, Pp 367-368.
- Lowder, W. and Beck, H. 1966.** Cosmic ray ionization in the lower atmosphere. *Journal of geophysics* **71**(190), Pp 4651-4659.
- Malance, A., Gaidolfi, L., Pessina, V. and Dallara, G. 1996.** Distribution of  $^{226}\text{Ra}$ ,  $^{232}\text{Th}$ , and  $^{40}\text{K}$  in soils of Rio Grande do Norte, Brazil. *J. Environmental Radioactivity*. **30**, Pp 55–67.
- Malanka, A., Pessina, V., Dallara, G. 1993.** Assessment of the natural radioactivity in the Brazilian state of Rio Grande, *Health Physics* **65**(3), Pp. 298-302.
- Mangala, J. M. 1987.** A multi-channel X-ray fluorescence analysis of fluorspar ore and rock from Mrima hill, Kenya, MSc Thesis, University of Nairobi.

- Mbuzukongira, P. 2006.** Assessment of occupational radiation exposures of artisan miners of Columbite-tantalite (Coltan) in the Eastern Democratic Republic of Congo. MSc Thesis, University of Nairobi, Unpublished.
- McCall, G. J. H. 1958.** Geology of Gwasi area. Geology Survey of Kenya Department, Report number 45.
- Merker, M., Light, E.S., Verschell, H.J., Mendell, R.B., Korff, S.A. 1973.** Time dependent worldwide distribution of atmospheric neutrons and their products (1) Fast neutron observation. *Journal of Geophysics.* **78(16)**, Pp 2727-2740.
- Mujahid. A, Hussain, S, Dogar, H. Karim. S. (2005)** “Determination of porosity of different materials by radon diffusion”, Physics radiation division, PINSTECH. P.O. Nilore, Islamabad, Pakistan, *Radiation Measurements* 40:
- Mustapha, A. O., Narayana, D.G.S., Patel, J.P. and Otwoma, D. (1997).** Radioactivity in some building materials in Kenya and contribution to the indoor external doses, *Radiation protection dosimetry.* 71(1) 65-69.
- Mustapha, A. O. 1999.** Assessment of human exposures to natural sources of radiation in Kenya. Ph.D Thesis, University of Nairobi.
- Mbuzukongira, P., Mustapha, A.O. and Mangala, M. J. 2007.** Occupational radiation exposures of artisans mining Columbite-tantalite in the eastern Democratic Republic of Congo, *J. Radiological Protection.* **27**, Pp 187-195.
- Mustapha, A.O., Patel, J.P. and Rathore, I.V.S. 2002.** Preliminary report on radon concentration in drinking water and indoor air in Kenya. *Environmental Geochemistry and health.* **24(4)**, Pp 387-396.

- National Council on Radiation Protection (NCRP). 1993.** Limitation of exposure to ionizing radiation, NCRP Report, **116**, Bethesda, MD.
- Nazaroff, W. W. and Nero jr, A. V. 1988.** Radon and its decay products in air. Wiley, New York. Pp 67-68
- O' Brien, K. 1978.** A code for the calculation of cosmic ray propagation in the atmosphere. *Health and safety laboratory*, EML 338 Report, New York.
- Odumo, B. O. 2009.** Radiological survey and elemental analysis in the gold mining belt, southern Nyanza, Kenya, M.Sc Thesis, University of Nairobi.
- Ohde S. (2004).** “Instrumental neutron activation analysis of carbonatites from Homa hills”, *Journal of Radioanalytical and Nuclear chemistry*. 3, Pp 214-221.
- Orgun, Y., Altinsony, N., Gultekin, A.H., Karahan, G., Celebi, N. 2005.** Natural radioactivity levels in granitic plutons and ground waters in Southeast part of Eskisehir, Turkey, *Applied Radiation and Isotopes*. **63**, Pp 267-275.
- Otwoma, D and Mustafa, A.O. 1998.** Measurement of  $^{222}\text{Rn}$  concentration in Kenyan ground water, *Health Physics*. 74 (1), 91-95.
- Patel, J. P. 1991.** Environmental radiation survey of the area of high natural radioactivity of Mrima hill of Kenya. *Discovery and innovation*, **3(3)**, Pp 31-36.
- Qureshi, A. A., Kakar, D. M., Akran, M., Khattak, M. T., Mehmood, K. and Khan, H. A. 2000.** Radon concentrations in coal mines of Baluchistan, Pakistan. *Journal of Environmental Radioactivity*, **48**, Pp 203-209.

**Rothkamm K. 2003.** Evidence for a lack of DNA double-strand break repair in human cells exposed to very low x-ray doses - Proceedings of the National Academy of Science of the USA, Pp 5057-5062.

**Rodriguez, L., Ruiz, E., Alonso, A. J. and Rincon, J. 2009.** Heavy metal distribution and chemical speciation in tailings and soils around a Pb-Zn mine in Spain. *Journal of environmental management*, **90**, Pp 1106-1116.

**Saggerson, E. P. 1957.** Geology of the Kitui south area. Kenya Geological Survey. Report number **37**.

**Sanders, L. D. 1954.** Geology of the Kitui area. Kenya Geological Survey. Report Number **30**.

**Shamos, M.H. and Liboff, A.R. 1966.** A new measurement of the intensity of cosmic ray ionization at sea level, *Journal of Geophysics*. **71(19)**, Pp 4651-4659.

**Singha Surinder., Asha Rania and Rakesh Kumar Muhajanb (2005).** “<sup>226</sup>Ra, <sup>232</sup>Th and <sup>40</sup>K analysis in soil samples from some areas of Punjab and Himachal Pradesh, India using gamma ray spectrometry” *Radiation measurements* 39, Pp 165-167.

**Singh, S., Singh, B., Kumar, A., (2003).** “Natural Radioactivity measurements in soil samples from Hamirpur district”, *Radiation Measurement* 36:

**Solon, L., Lowder, W and Blatz, H. 1980.** Investigations of natural environmental radiation. *Science*: **131**, Pp 903.

**Speer, J., Solberg, T and Becker, S. 1981.** Petrography of uranium bearing minerals of the Liberty Hill Pluton. South Carolina: phase assemblages and migration of uranium in granitoid rocks. *Economical Geology*: Pp 110-120.

**Tsai, T. L., Lin, C. C., Wang, T. W and Chu, T. C. 2008.** Radioactivity concentrations and dose assessment for soil samples around a nuclear power plant IV in Taiwan. *Journal of Radiological Protection*, **28**, Pp 347-360.

**Tzortzis, M., Svoukis, E. and Tsertos, H. 2004.** A comprehensive study of natural gamma radioactivity levels and associated dose rates from surface soils in Cyprus. *Radiation Dosimetry*, **109**, Pp 217-224.

**United Nations Scientific Committee on the Effects of Atomic Radiation (UNSCEAR). 1998.** Sources and effects of ionization radiation Report to the General Assembly, with Scientific Annexes B: Exposures from Natural Radiation Sources (New York: UNSCEAR), Pp 234-238.

**United Nations Scientific Committee on the Effects of Atomic Radiation (UNSCEAR). 2000.** Sources, effects and risks of ionization radiation, Report to The General Assembly, with Scientific Annexes B: Exposures from Natural Radiation Sources (New York: UNSCEAR), Pp 678-679.

**United Nations Scientific Committee on the Effects of Atomic Radiation (UNSCEAR). 2008.** Sources and Effects of Ionizing Radiation, Report of the United Nations Scientific Committee on the Effects of Atomic Radiation, Fifty-sixth session, New York, USA, Pp 456-458.

**Varley, N. R. and Flowers, A. G. 1998.** Indoor radon prediction from soil gas measurements. *Health Physics*, **74**, Pp 714-718.

**Veigaa, R. N., Sanchesa, R. M., Anjosa, K., Macarioa, J., Iguatemya, J.G., Aguiarb, A.m.A., Santosb, B., Mosqueraa, C., Carvalhoa, M and Baptista Filhoa, N.K. (2006)** “Measurement of natural radioactivity in Brazilian beach sands”, *Radiation Measurements*, Pp 346-349.

**Wikipedia.org/wiki/soapstone., Soapstone, 22/09/09.**

**Wong, M. H. 2003.** Ecological restoration of mine degraded soils with emphasis on metal contaminated soils. *Chemosphere*, **50**, Pp 775-780.

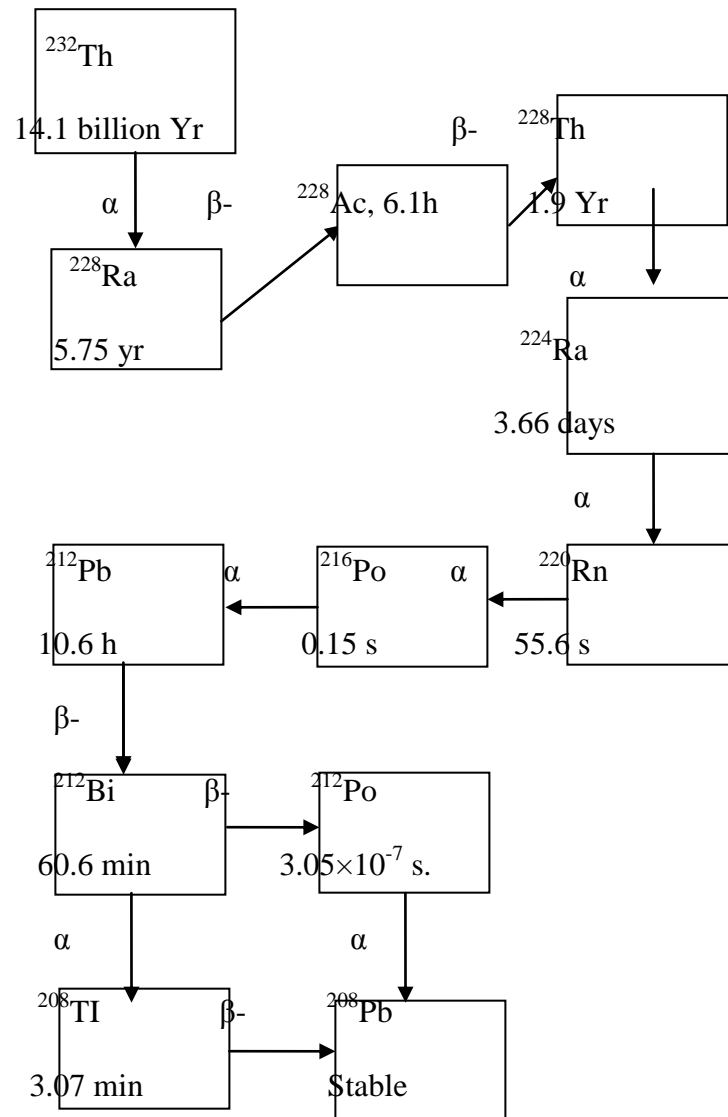
**Wong, J. W. C., Ip, C. M and Wong, M. H. 1998.** Acid forming capacity of Pb-Zn mine tailings and its implications for mine rehabilitation. *Environmental Geochemistry*, **20**, Pp 149-155.

**Xinwei, L., (2005).** “Radioactive Analysis of Cement and its Products collected from Shaanxi”, China. *Health Physics*. 88(1):

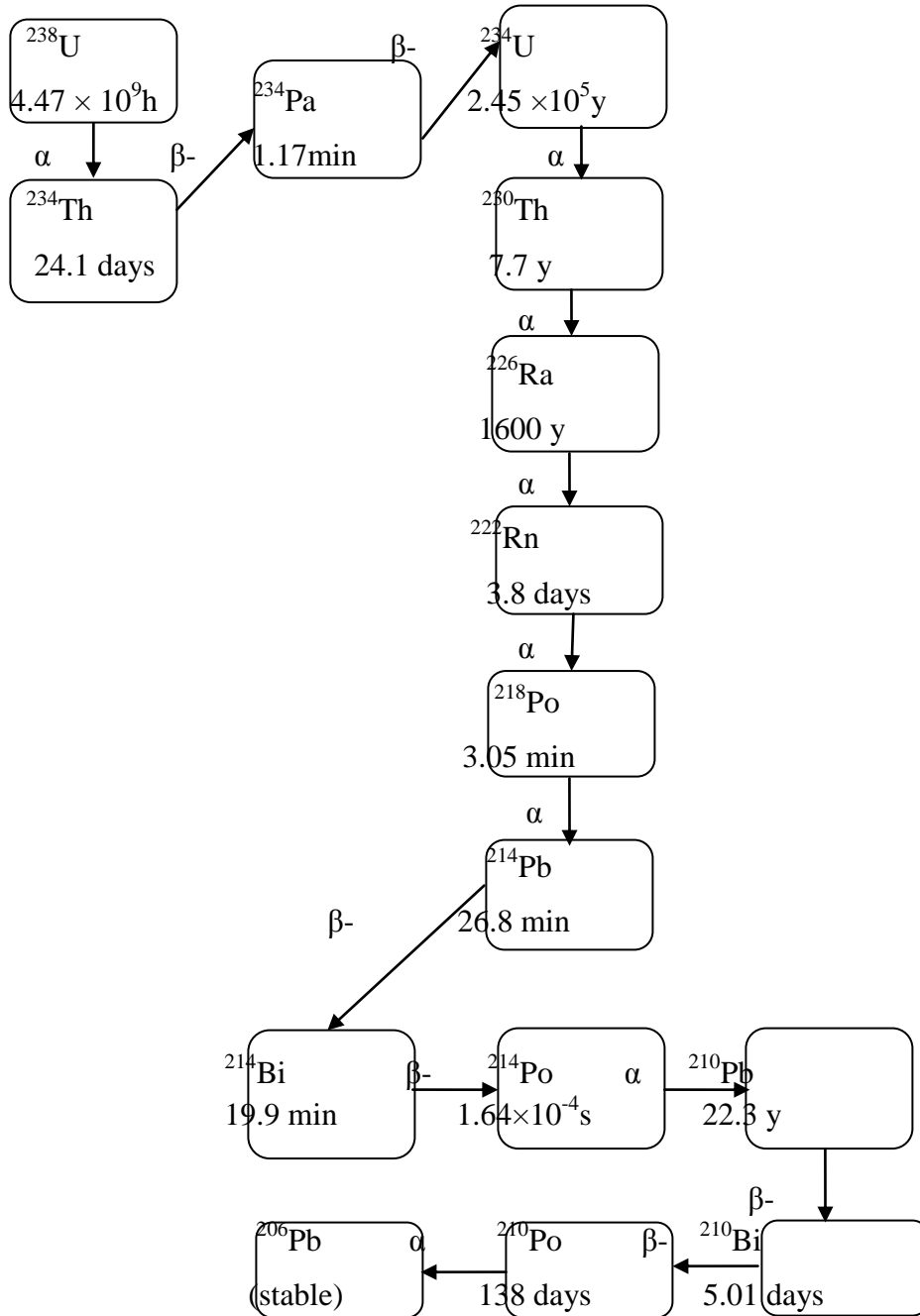
**Yang, Y., Wu, X., Wang, W., Lu, J. 2005.** Radioactivity concentrations in soils of the Xiazhuang granite area China. *Applied Radiation and Isotopes*. **63**, Pp 225-259.

## APPENDICES

### A1: Thorium series



## A2: Uranium series



**A3: Nuclide identification reports table**

Quarry name, sample depth.	Nuclide name	Absolute emission probability of gamma decay (%) ± 0.005	Energy ± 0.005 (keV)	Activity ± 0.005 (Bqkg <sup>-1</sup> )
Orengé 0.3m	<sup>40</sup> K	10.67	1460.81	587.00
	<sup>137</sup> Cs	85.12	661.65	2.52
	<sup>212</sup> Bi	11.80	727.17	35.10
	<sup>212</sup> Pb	44.60	238.63	52.90
	<sup>214</sup> Bi	46.30	609.31	35.50
	<sup>214</sup> Pb	37.20	351.92	37.10
	<sup>228</sup> Ac	27.70	911.60	59.50
	<sup>235</sup> U	54.00	185.71	9.41
Orengé 3m	<sup>40</sup> K	10.67	1460.81	1780.00
	<sup>212</sup> Bi	11.80	727.17	17.70
	<sup>212</sup> Pb	44.60	238.63	29.90
	<sup>214</sup> Bi	46.30	609.31	20.20
	<sup>214</sup> Pb	37.20	351.92	22.90
	<sup>228</sup> Ac	27.70	911.60	37.20
	<sup>235</sup> U	54.00	185.71	5.76
	Orengé 5m	<sup>40</sup> K	10.67	1460.81
<sup>214</sup> Bi		46.30	609.31	27.10
<sup>214</sup> Pb		37.20	351.92	25.10
<sup>228</sup> Ac		27.70	911.60	38.60
<sup>235</sup> U		54.00	185.71	5.35

Nyaberi 4m	<sup>40</sup> K	10.67	1460.81	307.00
	<sup>212</sup> Bi	11.80	727.17	68.10
	<sup>212</sup> Pb	44.60	238.63	95.50
	<sup>214</sup> Bi	46.30	609.31	37.60
	<sup>214</sup> Pb	37.20	351.92	38.20
	<sup>228</sup> Ac	27.70	911.60	99.70
	<sup>234</sup> Pa	0.59	1001.03	187.00
	<sup>235</sup> U	54.00	185.71	9.94
Nyaberi 7m	<sup>40</sup> K	10.67	1460.81	1020.00
	<sup>212</sup> Bi	11.80	727.17	23.90
	<sup>212</sup> Pb	44.60	238.63	36.40
	<sup>214</sup> Bi	46.30	609.31	24.50
	<sup>214</sup> Pb	37.20	351.92	28.00
	<sup>228</sup> Ac	27.70	911.60	39.90
	<sup>235</sup> U	54.00	185.71	6.39
	Ouma 1m	<sup>40</sup> K	10.67	1460.81
<sup>211</sup> Bi		1.20	351.10	72.80
<sup>212</sup> Bi		11.80	727.17	31.20
<sup>212</sup> Pb		44.60	238.63	43.80
<sup>214</sup> Bi		46.30	609.31	26.00
<sup>214</sup> Pb		37.20	351.92	23.90
<sup>228</sup> Ac		27.70	911.60	45.80
<sup>231</sup> Th		18.70	26.64	18.50
<sup>234</sup> Pa		0.59	1001.03	136.00
<sup>235</sup> U		54.00	185.71	6.41

Ouma 4m	<sup>40</sup> K	10.67	1460.81	813.00
	<sup>212</sup> Bi	11.80	727.17	19.30
	<sup>212</sup> Pb	44.60	238.63	29.90
	<sup>214</sup> Bi	46.30	609.31	29.90
	<sup>214</sup> Pb	37.20	351.92	33.40
	<sup>228</sup> Ac	27.70	911.60	44.70
	<sup>235</sup> U	54.00	185.71	6.16
Ouma 8m	<sup>22</sup> Na	99.94	1274.54	0.48
	<sup>40</sup> K	10.67	1460.81	744.00
	<sup>212</sup> Bi	11.80	727.17	57.40
	<sup>212</sup> Pb	44.60	238.63	98.00
	<sup>214</sup> Bi	46.30	609.31	72.40
	<sup>214</sup> Pb	37.20	351.92	77.60
	<sup>226</sup> Ra	3.28	186.21	210.00
	<sup>228</sup> Ac	27.70	911.60	103.00
	<sup>231</sup> Th	18.70	26.64	26.80
	<sup>235</sup> U	54.00	185.71	12.80
Barongo 0.3m	<sup>40</sup> K	10.67	1460.81	641.00
	<sup>137</sup> Cs	85.12	661.65	1.74
	<sup>212</sup> Bi	11.80	727.17	34.80
	<sup>212</sup> Pb	44.60	238.63	56.40
	<sup>214</sup> Bi	46.30	609.31	39.10
	<sup>214</sup> Pb	37.20	351.92	39.10
	<sup>228</sup> Ac	27.70	911.60	66.40
	<sup>231</sup> Th	18.70	26.64	24.00
	<sup>234</sup> Pa	0.59	1001.03	119.00
	<sup>235</sup> U	54.00	185.71	8.53

Barongo 4m	<sup>40</sup> K	10.67	1460.81	245.00
	<sup>211</sup> Bi	1.20	351.10	92.80
	<sup>212</sup> Bi	11.80	727.17	5.75
	<sup>212</sup> Pb	44.60	238.63	81.80
	<sup>214</sup> Bi	46.30	609.31	30.60
	<sup>214</sup> Pb	37.20	351.92	30.40
	<sup>228</sup> Ac	27.70	911.60	84.60
	<sup>231</sup> Th	18.70	26.64	23.50
	<sup>234</sup> Pa	0.59	1001.03	214.00
	<sup>235</sup> U	54.00	185.71	7.86
Barongo 8m	<sup>40</sup> K	10.67	1460.81	1090.00
	<sup>212</sup> Bi	11.80	727.17	23.30
	<sup>212</sup> Pb	44.60	238.63	30.10
	<sup>214</sup> Bi	46.30	609.31	29.30
	<sup>214</sup> Pb	37.20	351.92	28.80
	<sup>226</sup> Ra	3.28	186.21	120.00
	<sup>228</sup> Ac	27.70	39.30	39.30
	<sup>234</sup> Pa	0.59	1001.03	66.60
	<sup>235</sup> U	54.00	185.71	7.28
British 0.3m	<sup>40</sup> K	10.67	1460.81	883.40
	<sup>137</sup> Cs	85.12	661.65	34.30
	<sup>212</sup> Bi	11.80	727.17	35.20
	<sup>212</sup> Pb	44.60	238.63	78.70
	<sup>214</sup> Bi	46.30	609.31	34.30
	<sup>214</sup> Pb	37.20	351.92	38.40
	<sup>228</sup> Ac	27.70	911.60	42.30
	<sup>231</sup> Th	18.70	26.64	26.40
	<sup>235</sup> U	54.00	185.71	8.53

British 1m	<sup>40</sup> K	10.67	1460.81	284.00
	<sup>212</sup> Bi	11.80	727.17	62.70
	<sup>212</sup> Pb	44.60	238.63	103.00
	<sup>214</sup> Bi	46.30	609.31	39.30
	<sup>214</sup> Pb	37.20	351.92	42.70
	<sup>228</sup> Ac	27.70	911.60	106.00
	<sup>231</sup> Th	18.70	26.64	32.50
	<sup>234</sup> Pa	0.59	1001.03	198.00
	<sup>235</sup> U	54.00	185.71	11.10
British 15m	<sup>40</sup> K	10.67	1460.81	403.00
	<sup>212</sup> Bi	11.80	727.17	52.30
	<sup>212</sup> Pb	44.60	238.63	86.40
	<sup>214</sup> Bi	46.30	609.31	33.00
	<sup>214</sup> Pb	37.20	351.92	32.80
	<sup>228</sup> Ac	27.70	911.60	97.80
	<sup>235</sup> U	54.00	185.71	9.77